



Potential for constraining sequence stratigraphy and cycle stratigraphy with U-Pb dating of carbonates

E. Troy Rasbury ^{a,*}, Gavrin Piccione ^b, William Hofst ^a, W. Bruce Ward ^c

^a Department of Geosciences, Earth and Space Sciences 255, Stony Brook University Stony Brook, NY 11794-2100, USA

^b Earth and Planetary Sciences, University of California Santa Cruz, 1156 High Street, Santa Cruz, CA 95064, USA

^c e4Sciences, PO Box 178, Newtown, CT 06470, USA



ARTICLE INFO

ABSTRACT

Keywords:
U-Pb carbonates
Hydrologic realm
Carbonate petrography
Sequence boundaries
Diagenesis

Studies of sequence stratigraphy and cycle stratigraphy in carbonate formations increasingly improve our understanding of depositional systems and basin to global correlations. However, there is still a scarcity of dated sequences to determine the time length of sequences and cycles. The durations of sequences and cycles provide tests of the processes that produce them. Poor age resolution mostly stems from the lack of recognizable volcanic ash deposits in many sections. Through continuing advances in analytical techniques and approaches to sampling, the current state of U-Pb dating of carbonate sedimentary rocks provides opportunities to fill in age gaps. The approach should build on well-constrained 3-dimensional stratigraphic architectures and diagenetic stratigraphies.

Over the last 10 years there has been an explosion in the application of U-Pb dating of carbonates with the introduction of Laser Ablation (LA) ICPMS analyses. What these studies show is that measured carbonate ages are often younger than the age of deposition and in many cases, multiple ages are derived from individual samples, indicative of multiple events. Often these younger events can be tied to known tectonic activity or sea level changes that would have influenced hydrology, perhaps bringing in new reactive fluids to dissolve or replace some existing minerals and precipitate new minerals. U-Pb dating of carbonates offers unprecedented potential to work out the timing of deposition and diagenesis in carbonate sequences. As more samples are investigated, particularly in the context of field, petrographic, and geochemical constraints, our views on how to sample and the reliability of ages will be strengthened. Additionally, as more primary and secondary natural reference materials with different textures and mineralogy are made available, our ability to evaluate the reliability of LA ICPMS ages of unknowns will improve. While ages of U-Pb carbonate will likely never approach the precision of U-Pb zircon and Ar-Ar sandstone dating of tuffs, carbonates have the advantage of being abundant in space and time, often occurring where volcanic ash deposits are not recognized.

Here we review geochronology from Carboniferous-Permian cyclothems that have been shown in numerous studies to be driven by glacio-eustacy, presumably paced by Milankovitch cycles, and that can be understood in a sequence stratigraphic framework. We compare U-Pb carbonate ages with other radiometric ages and biostratigraphy to demonstrate the reliability of the carbonate ages and thus highlight potential. We show new Laser Ablation U-Pb Carbonate data for a particularly well-studied paleocean carbonate with outstanding U-Pb systematics and compare with published isotope dissolution ages, particularly focusing on the power of the image-based approach to carbonate dating advanced by Drost et al. (2018). Finally, we compare results between U-Pb zircon dating and U-Pb carbonate dating of cyclothems with Bayesian modeling and conclude that numerous older precision dates throughout a stratigraphic section provide age constraints that can be similar in precision to a few highly precise ages, depending on the stratigraphic distribution throughout the section.

* Corresponding author.

E-mail address: troy.rasbury@stonybrook.edu (E.T. Rasbury).

1. Introduction

The questions we are asking of the rock record create a great demand for improved time resolution. This demand is highlighted by the National Academies 'A Vision for NSF Earth Sciences 2020-2030: Earth in Time' (2020), which describes a need for better temporal constraints to test geological models. This is especially true in the carbonate rock record, and for sequence stratigraphic architectures. Sequence stratigraphy and cycle stratigraphy in carbonate formations increasingly reveal information about temporal and spatial changes in depositional environments, and push our understanding of potential drivers, such as eustatic sea level. However, there is still a scarcity of geochronological constraints to test cycle durations and provide constraints on rates of sedimentation. Through continuing advances in analytical techniques and approaches to sampling, the current state of U-Pb dating of carbonates makes the goal of widespread absolute dating of carbonate stratigraphy more possible than ever before. These advances occur on the back of decades of U-Pb developments and well over a century of developing concepts of carbonate sequence stratigraphy (before it was called that). We briefly review this history to provide context for current advances and suggest directions for future applications of carbonate geochronology to sequence stratigraphy.

A significant portion of shelf carbonates, if not all, preserve rhythms of deposition recorded by 3-dimensional facies distributions. Superposition, cross cutting relocations and stratigraphic changes in vertical thicknesses and lateral facies distributions define cycles of many scales commonly with multifaceted hierarchies. Such facies in Late Paleozoic cyclothems have been recognized and studied for over a century (e.g., [Fielding 2021](#); [Montanez, 2022](#); [Wanless and Shepard, 1936](#)). During the 1950s through 1970s with improved understanding of carbonate facies, cycles and sequences were increasingly recognized in most platform carbonates, as exemplified in the syntheses of [Wifilson \(1975\)](#). At this time, it was realized that the facies distribution and extent of carbonates are sensitive to sea level and follow the 'principle of fast but rapid deposition' such that carbonate strata are likely dominated by periods of non-deposition ([Wifilson, 1975](#)).

The advent of seismic sequence stratigraphy fueled the use of onlap and offlap of strata to provide a record of regional sea level change ([Vail et al., 1977](#)). By comparing basins across the globe it appears possible to pull out the eustatic signal (e.g. [Haq and Schutter, 2008](#)). Using seismic biostratigraphy and onlap-offlap sequences, [Ross and Ross \(1985\)](#) argued that Late Paleozoic 1–5 Ma sequences responded to eustatic changes in sea level and were 'synchronous and world-wide'.

After refinements by [Van Wagoner et al. \(1988\)](#), use of sequences and terminology to describe the components became more widespread. Sequence stratigraphic analysis on carbonate rocks reached a renewed level that continues to the present. During this time, two of many important points with respect to this paper became more recognized. 1) The different scales of stratigraphic packaging or architecture were defined by 3-dimensional cycles and that single vertical sections alone are insufficient to define the cyclicity (e.g. [Kerans and Tinker, 1997](#)). 2) The packaging of the cycles differs during icehouse and greenhouse times ([Read et al., 1995](#); and see [Montanez, 2022](#); [Fig. 4](#) for current view).

By 2000, our level of understanding of hierarchical cycles in carbonates was becoming quite sophisticated. This understanding was dependent on sea-level curves and proxies which have become increasingly better understood. Correlations, biostratigraphy, chemostratigraphy and sea level trends were and are determined from carbonate strata and carbonate minerals. However, most sequences were undated so that scales of cycles and global correlations were untested by geochronology. The Carboniferous-Permian boundary as an excellent example that is pertinent to this paper. [Harland et al. \(1990\)](#) Geologic Timescale reported the Carboniferous-Permian boundary at 290 ± 20 Ma (2σ), an uncertainty that precludes answering many questions we ask of the stratigraphic record, let alone of any meaningful time

analyses.

Prior to the mid 1980's radiometric age dates for carbonate strata older than Paleocene were on minerals in ashes, volcanic layers, and intrusions. The earliest work on dating carbonates used Pb-Pb to date Archean stromatolites ([Moore et al., 1987](#)). While the Pb-Pb was later shown to likely result from Pb mineralization and was thus not a primary age ([Sumner and Bowring, 1996](#)), this spurred the first U-Pb carbonate race, as a number of papers using U-Pb followed and showed the great potential for providing improved time constraints (summarized in [Rasbury and Cofle, 2009](#)). This earlier work used isotope dilution (ID) which is time consuming and lacks opportunities for prescreening for favorable samples, which slowed advances. Determining which samples might work was improved somewhat with imaging techniques like phosphor imaging ([Cofle et al., 2003](#)), but high uranium is not the only key to success and this imaging did not address the Pb content.

LA ICPMS (Laser Ablation Inductively Coupled Plasma Mass Spectrometry) analyses of carbonates has greatly expanded the potential for identifying datable carbonates. This technique, established by Randy Parrish at NIGL (British Geological Survey NERC Isotope Geosciences Laboratory) set the stage for a new revolution in U-Pb dating of carbonates. The first analysis using LA ICPMS to date carbonates was published in 2014 ([Li et al., 2014](#)) in a study aimed at constraining Jurassic stratigraphy. In this case the biostratigraphy was good enough to recognize that the dated cements were too young to represent the time of deposition. However, the study highlighted the great potential for LA ICPMS to date carbonates. Since that first contribution, datasets of data reduction and reference materials are still being ironed out, but numerous labs are participating in the effort. Laser Ablation ICPMS dating of carbonates was highlighted during the 2018 Goldschmidt Conference, a workshop on LACarb, which we adopt as a short title for laser ablation U-Pb dating of carbonates here. The LACarb website maintains an extensive bibliography of LACarb work since 2014 (<https://la-carb.com>), and welcomes researchers to join this group. Much of the recent application of LACarb has been on carbonate mineral filling fractures, in efforts related to unravelling later fluid flow and tectonic events, recently summarized by [Roberts and Holdsworth \(2022\)](#).

Initial LACarb techniques did not solve many of the issues of sample selection needed for widespread application to carbonate stratigraphy. Carbonates are soluble in many solutions and subject to alteration through time. Some of these features are too subtle to be easily recognized with conventional petrography. Many of these issues are solved with an exciting development in LACarb using an image based approach to pooling pixels ([Drost et al., 2018](#)) and a follow up of this using robust regression of all of the data ([Hoareau et al., 2021](#); [Rochín-Bañaga et al., 2021](#)), which we will refer to as the Drost method. This approach is particularly appealing for labs using a quadrupole mass spectrometer because pixels can be selected by criteria such as element concentrations or ratios. Often carbonates have distinctive compositions (high Mg or low Mg calcite, dolomite etc.) and trace element compositions that can be understood in the framework of the hydrogeological system(s) that formed them. For carbonates, which are vulnerable to diagenetic change, this ability to visualize element maps in the context of petrography offers a huge advance not only for dating, but also for deciphering more about the fluids that formed and/or altered them.

2. Environmental controls on U and Pb in carbonates

2.1. Syn-sedimentary carbonates

Syn-depositional carbonates form in marine, terrestrial and transitional environments. A major bottleneck for U-Pb dating is recognizing conditions that produce relatively high and variable U-Pb ratios ([Rasbury and Cofle, 2009](#)). While early work focused more on the U content of carbonates ([Amiel et al., 1973](#); [Chung and Swart, 1990](#); [Cofle et al., 2003, 2004](#); [Gvirtzman et al., 1973](#); [Haglund et al., 1969](#); [Hoff](#)

et al., 1995; Lahoud et al., 1966; Rasbury et al., 2000; Schroeder et al., 1970), it is equally important to understand Pb concentrations (and thus the U/Pb ratios) for U–Pb dating (Rasbury et al., 2021; Rasbury and Cofle, 2009; Woodhead et al., 2006). Understanding the geochemistry of the fluids that are responsible for carbonate precipitation is key to predicting what types of carbonates hold potential for U–Pb dating. Though, using existing chemical constraints published on carbonates to assess potential samples amenable for dating is complicated by the fact that U is not typically reported in carbonates except for dating (we want to change that) and unsuccessful attempts at dating commonly go unreported. Below we provide ideas on geochemical characterization of carbonates sorted by depositional environment, which can serve as a foundation from which to build a more comprehensive database of environmental conditions that most typically produce carbonates with favorable U–Pb ratios.

Rasbury and Cofle (2009) reviewed U–Pb dating of carbonates in the context of the hydrologic realms that these carbonates were formed in. At about that time, U–Pb dating of speleothems by Multi-Collector ICPMS (MC-ICPMS) was gaining momentum (Woodhead et al., 2006, 2012; Woodhead and Pfickerling, 2012). Woodhead et al. (2006) showed that screening approaches that had been used for U-series dating were also helpful for identifying favorable samples for U–Pb dating. This is because Pb and Th are both mostly insoluble in surface fluids. Even with this predictive approach, finding samples with favorable U/Pb can be difficult, but laser ablation methods offer an exciting avenue to not only date rocks, but to learn fundamental details of the geochemistry in the context of these ages. As more samples are analyzed in the context of detailed stratigraphy, and with an eye towards how these samples reflect the fluids that formed them, important patterns will emerge that will further refine approaches to carbonate dating.

2.2. Marine carbonates

Marine carbonate components have evolved through time due to biological evolution and evolution of ocean chemistry. This includes the dominant mineralogy of skeletal material at any one time (Pomar and Hafllock, 2008; Stanley and Hardie, 1998). Marine cements and skeletal calcium carbonates include aragonite, low-Mg calcite, and high-Mg calcite. Carbonates in modern marine environments are dominantly aragonite and high-Mg calcite, low Mg calcite is only dominate in deep cold waters. The major mineralogy plays a role in U incorporation into the carbonates. Aragonite does not exclude U, while calcite does (Reeder et al., 2000).

It has been shown that the major ion composition of seawater has fluctuated through the Phanerozoic (Dickson, 2002; Hardie, 1996; Horita et al., 2002; Lowenstein, 2001). Changes in the Mg/Ca of seawater appears to have dictated whether the favored calcium carbonate was aragonite (high Mg/Ca seawater) or calcite (low Mg/Ca seawater) (Hardie, 1996). Importantly, these major cycles appear to correspond to icehouse (high Mg/Ca) and greenhouse (low Mg/Ca) periods on Earth. Certainly the correspondence between times of aragonite seas producing $MgSO_4$ evaporites, versus times of calcite seas producing KCl evaporites in between salts strongly implicates secular changes in major ions in seawater, rather than some other control such as atmospheric pCO_2 (Hardie, 1996). Hardie (1996) used a simple assumption that seawater is a two-component mix between river waters and fluids emerging at the Mid Ocean Ridge (MOR) after interacting with and alterting oceanic crust. Small changes in the seawater flux through the MOR can predict the fluctuating Mg/Ca ratio (Hardie, 1996), but additional constraints must be imposed to account for K, which does not appear to change through time (Demicco et al., 2005). Other studies have downplayed the importance of MOR circulation and find that during times of high sea level more carbonates are dolomitized, driving sea water to lower Mg concentrations, and more evaporites form on the shelves, driving sea water to lower sulfate concentrations (Holland et al., 1996). It is also true that as seawater changes, so do the

reactions along the pathway in the MOR (Antonellini et al., 2017) and on the shelf. Models for secular changes in seawater will be improved, but importantly, work from Cenozoic aragonitic corals (Denniston et al., 2008; Getty et al., 2001; Gothmann et al., 2019) shows an increase in U through the Cenozoic as the Earth moved from calcite seas into aragonite seas (Fig. 1). While part of this increase could simply result from decreasing Ca concentrations, this cannot account for all of the change (Gothmann et al., 2019).

Marine cements from the Carboniferous-Permian have U concentrations comparable to the Neogene, consistent with U reflecting secular change (Fig. 1). We suggest that times of aragonite seas, like today, the Late Paleozoic, and the Neoproterozoic, may have elevated U in carbonates, and conversely, times of calcite seas likely have lower U in carbonates because a main control is the U/Ca ratio of the parent fluid. The major mineralogy also plays a role in U incorporation into the carbonates (Reeder et al., 2000). This makes the shift to more elevated U concentrations into the Neogene aragonite seas even more significant as aragonite formation would sequester more U and would drive a downward trend. Interestingly, Sr also shows a trend with these major cycles (Steuber and Vezier, 2002) that is opposite that of U. Trace elements are powerful proxies for process because they do not control the system, they simply respond to it. As more detail becomes available for U in marine carbonates, we expect that the drivers will be revealed.

Aragonite is metastable and will dissolve or be replaced by low Mg calcite by dissolution and re-precipitation processes. Understanding the details, especially the timing, of these changes is key to identifying sedimentary carbonates that can be dated by U–Pb to provide the age of deposition. Rasbury et al. (2004) showed that marine cements from the Late Carboniferous, which were aragonite altered to calcite, formed soon after deposition and preserved elevated U concentrations despite neomorphic conversion to calcite. Similar neomorphosed marine cements from the Permian Reef Complex of West Texas and New Mexico provided the WC-1 reference material for LACarb dating (Roberts et al., 2017).

2.3. Terrestrial carbonates

Carbonates formed in terrestrial environments are far less predictable than marine environments because water chemistry varies widely depending on the regional geology and hydrology. Speleothem deposits have been a target for U-series dating and a summary of the prospects for U–Pb dating can be found in review papers such as Woodhead and Pfickerling (2012). Speleothems form from meteoric diagenesis, and this has been well covered elsewhere (e.g. Woodhead et al., 2006). Basically, the layering of speleothems and the ability to date them provides important details of the climate at the time of formation, but they often form much later than the time of deposition of the rocks they occur within. Calcite (calcite) is another meteoric product that forms at subaerial exposure. This too can be much later than the time of actual deposition, and age uncertainties could be large due to the long-term exposure. For example Hoff et al. (1995) analyzed dolomites associated with subaerial diagenesis from the Pre Upper Permian Unconformity (PUPU) of the Wahoo Fm in the Brooks Range, Alaska, and obtained an age of 267 ± 31 Ma (2 σ). This age is consistent with the unconformity it formed on, but with an uncertainty that was as large as the expected duration of the exposure (30–40 m.y.). Winter and Johnson (1995) also dated dolomite associated with the major sequence boundary of the Sauk and Tippecanoe sequences in Wisconsin, USA and obtained an age of 504 ± 14 Ma (2 σ), entirely consistent with the biostratigraphic framework. These studies showed that U can be concentrated at sequence boundaries and set the stage for examining marine and terrestrial sequences with 4th (<0.5 m.y.) and 5th (<0.1 m.y.) order sequence boundaries (Brigaud et al., 2021; Kurumada et al., 2020; Rasbury et al., 1997, 1998, 2000, 2006; Wang et al., 1998).

Lakes may also be sites of prominent carbonate deposits, and the position and stacking patterns of lacustrine facies can be used to show

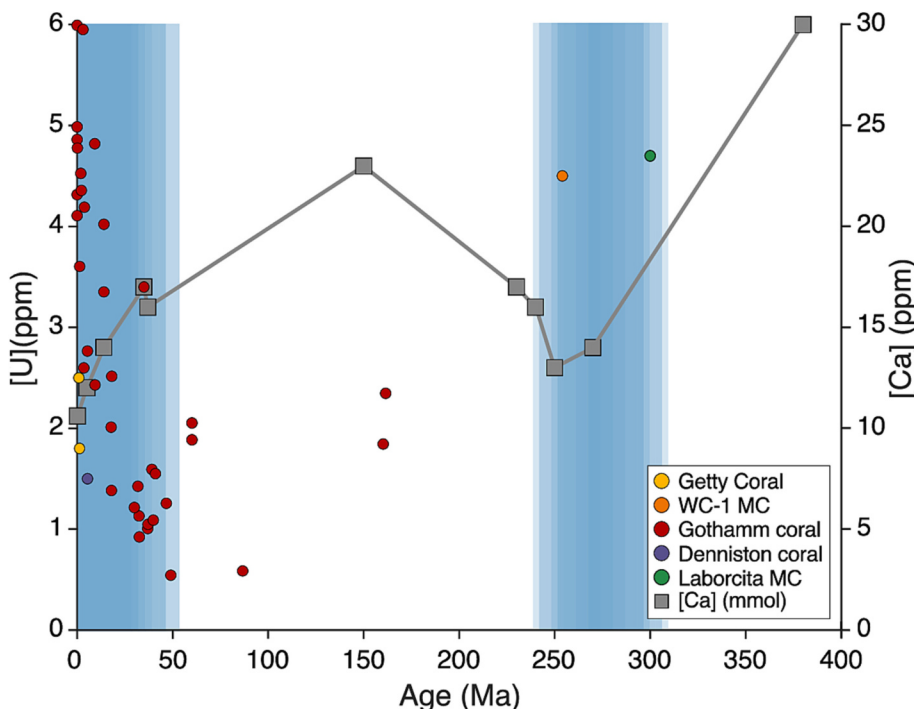


Fig. 1. U concentrations in corals and marine cements relative to time of aragonitic seas. Data are from Laborcita FAMC (former aragonite marine cement) from Rasbury et al. (2004), and WC-1 FAMC from Roberts et al. (2017). Coral aragonite data are from Getty et al. (2001), Denniston et al. (2008) and Gothmann et al. (2019). Blue shaded areas are the approximate time intervals of aragonite seas. The gradient in shading is intended to reflect the temporal uncertainties and gradation of these boundaries. Grey squares and curve represent Ca concentration data from fluid inclusions in evaporites (Horita et al. 2002). (For interpretation of the references to colour in this figure legend, the reader is referred to the web version of this article.)

changes in sea level that allows geologists to consider hydrogeological changes in the context of climate and tectonics (Carroll and Bohacs, 1999). Lacustrine carbonates from a variety of settings have been dated by U-Pb (Copley et al., 2005; Lawson et al., 2022; Montano et al., 2021, 2022; Piccione et al., 2022). A focus on the sea level chemistry and U incorporation in carbonates is sorely needed for better predictions of lacustrine samples amenable for U-Pb. This is especially true given that some lacustrine carbonates do not have favorable U-Pb ratios and any attempts to date them are unlikely to have been published.

A recent contribution from Montano et al. (2022) studied Late Cretaceous to Paleogene carbonate bearing lacustrine sequences in Argentina and showed that age models based on U-Pb zircon dating (LA ICPMS dating of detrital zircons to determine the Maximum Depositional Age (MDA)) compare quite favorably with those based on U-Pb dating of carbonates. Using careful petrography and an understanding of the carbonate facies that were being sampled, these authors considered all of the data obtained from each horizon using the MSWD of the population of isochron ages from each horizon to determine if the data met the criteria to be included. This work elegantly demonstrates the power of using LACarb for dating terrestrial sedimentary sequences and sets a bar that any studies that seek to improve stratigraphic time resolution should meet or exceed.

2.4. Transitional environments

Much of the alteration of marine carbonates occurs in transitional environments (e.g. Heckel, 1983). When sea level is rising or falling recently deposited sediments are subjected to different fluids, which are not necessarily in equilibrium with the marine deposits. The mixing zone between marine and freshwater, as well as the boundaries between the marine vadose and phreatic zones, move with transgression and regression seas (or lakes). Facets of diagenesis in the context of depositional packages are recorded in cements and dissolution events, and all of these changes can be considered in the framework of sequence stratigraphy (Morad and Ketzer, 2013). Carbonates produced in this context that can be dated with U-Pb will improve our understanding of the boundaries as well as improve age resolution of the sections they occur with (Table 1; at the end of the document).

3. Application of carbonate U-Pb constraints in sequence stratigraphy

3.1. Sequence stratigraphic boundaries

Sequence stratigraphy provides a framework from which to think about associated facies in the context of base level change, and the types of fluids (meteoric, seawater, etc.) that might have interacted with the deposits to alter depositional minerals and form new minerals throughout the evolution of a basin. Sequence boundaries are the fundamental surfaces that bracket systems tracts (transgressive, highstand, regressive, etc) and the details of these tracts provide insight into changes in accommodation space and/or sediment supply. Often, the sequence order can be defined, such as 3rd, 4th and 5th order cycles. Diagenesis such as hardground formation in starved deep-water transgressive systems tracts, or meteoric diagenesis (e.g. karst) and soil formation during subaerial exposure at low stands, can be profound. If the sequences are 4th (<0.5 m.y.) or 5th order (<0.1 m.y.) cycles, the duration of this alteration is typically smaller than the reasonably expected uncertainties in the ages of diagenetic minerals that formed as the surface was active (Brigaud et al., 2021; Rasbury et al., 1997). In detail, textures that appear to be early diagenesis can give ages that are significantly younger than the age of deposition (Brigaud et al., 2021; Israelson et al., 1996; Ift et al., 2014; Montano et al., 2022; Wang et al., 1998). Thus, in concert with field and petrographic observations, U-Pb dating of carbonates will reveal details of diagenetic fabrics that will improve how we understand the systems that created or altered them (Table 1).

3.2. An example: Carboniferous-Permian cyclothems

As originally defined in the Illinois Basin of North America, cyclothems represent high-amplitude and high-frequency changes in sea level that resulted in marine to non-marine packages with evidence for subaerial exposure (Wanless and Shepard, 1936). Wanless and Shepard (1936) made a case for the correlation of cyclothems globally and suggested that improved paleontology and other age constraints could help to refine these correlations. Following that work numerous studies have

Table 1

Summary of major diagenetic processes due to marine sequence stratigraphic controls with predicted carbonate cements and potential for U–Pb dating. Table modified from (Morad and Ketzer, 2013).

Processes and Products	Climatic/Setting	Predicted U–Pb	Potential for U–Pb dating	Reference/source
Sequence Boundaries				
Dissolution and karstification	Humid/subaerial	May provide a fluid with high U and/or flow of calcite	good	
Phreatic meteoric cementation	Subaerial	Depends on a source of U.	good	(Chung and Swart, 1990)
Dedolomitization	Subaerial	If the original dolomite was 'hot' it is possible the carbonate formed from it will have elevated U. However, the Fe oxides that often accompany this transformation have a high affinity for U and may make it unavaiable for the carbonate.	unknown but promising	
Pedogenesis and calcrete formation	Subaerial	Depends on a source of U but several examples show potential for calcite and dolomite at subaerial exposure surfaces. U-series work on pedogenic carbonate on alluvial gravels has high potential (Björnsjö et al., 2012; Björnsjö and Sharp, 2003; Fletcher et al., 2010, 2011; Gold et al., 2011, 2015; Rockwell et al., 2019; Sharp et al., 2003). Calcite found in association with calcretes may sequester U so that the calcite has unfavorable U–Pb (Hall et al., 2019; Langford, 1974).	good	(Hoff et al., 1995; Rasbury et al., 1998, 2000, 2006; Wang et al., 1998; Winter and Johnson, 1995).
Dolomitization from evaporation	Coastal	Evaporitic fluids are enriched in Mg and U, evaporative dolomites are frequently 'hot'.	good	(Luczaj and Goldstien, 2000).
Dolomitization from mixing fluids	Coastal	Seawater freshwater mixing zones can produce dolomite with	good	(Rasbury et al., unpublished; Florida aquifer)

Table 1 (continued)

Processes and Products	Climatic/Setting	Predicted U–Pb	Potential for U–Pb dating	Reference/source
Dolomitization	Marine	It is not clear that dolomite should have a stronger preference for U than calcite (which is very low). However, there are numerous examples of dolomite with elevated U and U–Pb and more work is needed to understand this.	good	(Elfissa et al., 2020).
Hardgrounds and firmgrounds	Marine	Carbonates that form on these types of surfaces appear to be very promising for U–Pb dating	good	(Brigaud et al., 2021).
Isopachous Mg-calcite and aragonite cements	Marine	These carbonates have a higher affinity for U than low-Mg calcite and depending on how the minerals are transformed or dissolved this is a potential source of U to newly formed calcite.	good	(Chung and Swart, 1990).
Dolomite and calcite cements	Mixed marine-meteoric	Seawater freshwater mixing zones can produce dolomite with reasonably high U and U–Pb	good	(Rasbury et al., unpublished; Florida aquifer)
Dissolution reflected to coals on TS and in early TST	Mixed marine-meteoric	If the minerals that are being dissolved have elevated U, this potentially provides U for the next generation of carbonate cements.	unknown	
Highstand systems tracts				
Mg-calcite and aragonite cements	Shallow marine	These carbonates have a higher affinity for U than low-Mg calcite and depending on how the minerals are transformed or dissolved this is a potential source of U to newly formed calcite.	good	Chung and Swart, 1990)
Dolomite and calcite cements	Mixed marine-meteoric	Dolomite and calcite are relatively stable carbonates. The U–Pb will	unknown	

(continued on next page)

Table 1 (continued)

Processes and Products	Climatic/Setting	Predicted U-Pb	Potential for U-Pb dating	Reference/source
Pressure dissolution	Marine	depend on source of U and details of the Kd (for dolomite).	unknown	
Mg-calcite and aragonite cements	Deep marine	This may provide a source of U for later carbonate cements.	unknown	
Meteoric dissolution	Meteoric or mixed	This may provide a source of U for later carbonate cements.	good	Chung and Swart (1990)
Transgressive systems tracts				
Mg-calcite and aragonite	Marine	These minerals are metastable but their formation provides a source of U for future carbonate cements.	good	Chung and Swart (1990); Rasbury et al. (2000)
Dolomitization (seawater)	Marine	It appears that dolomite may have a higher Kd for U than calcite. More work is needed on dolomite cements.	unknown but promising	(Efimova et al., 2020)

examined cycloths across basins and in agreement with Wanless and Shepard (1936) have shown that they represent high-amplitude (>100 m), likely glacio-eustatic changes in sea level. The magnitude and beat of these cycles offers a high resolution record of the waxing and waning of southern hemisphere glaciations (Crowell, 1978; Heckel, 2008). Paleontological studies allow refined cyclothem correlations globally (Davydov et al., 2010; Ross and Ross, 1985), and age constraints from ashes and paleosols have refined the initiation of glaciation, global correlations and cycle durations (Davydov et al., 2010; Eros et al., 2012; Pofontin et al., 2021; Rasbury et al., 1998). Within that framework, the initiation of glaciation in the Carboniferous may be defined by the earliest recognized cycloths (Bishop et al., 2009; Pfeiffenbarger and Frank, 2015; Smith and Fred Read, 2000; Wright and Vanstone, 2001) near the end of the Lower Carboniferous (within the Visayan). The end of Late Paleozoic glaciation may be defined by the end of high-amplitude high-frequency cycles (Safler et al., 1999), which occurs in the Lower Permian (within the Leonardian). Pfeiffenbarger (2021) reviewed cycloths specifically in the context of sequence stratigraphy and detailed the cycle orders, providing a foundation for global correlation. The duration of cycloths has been tested through radiometric age constraints (Davydov et al., 2010; Eros et al., 2012; Pofontin et al., 2021; Rasbury et al., 1998; Safler et al., 1999). It has long been recognized that Late Paleozoic Ice Age (LPIA) glacial centers shifted across the Gondwanan continents as this mega-continent moved across the south pole (Crowell, 1978; Wanless and Shepard, 1936). More recent studies provide radiometric dates for these glacial and glacio-marine deposits, confirming and refining this understanding of a dynamic system that shifted through time, rather than one large ice sheet that lasted from the beginning of the icehouse to the end (Dietrich et al., 2021; Griffis et al., 2019; Guibranson et al., 2010). Climate modeling for the LPIA suggests that eccentricity paced climate (Horton et al., 2012). A detailed paleosol proxy record for the LPIA shows swings in pCO_2 that correspond to the glacial-interglacial record from the southern hemisphere (Montañez et al.,

2007). The cyclothem record supports a dominant eccentricity control on LPIA climate (Montañez, 2022).

The character of cycloths reflects the latitude, climate and tectonic environment of deposition (Wanless and Shepard, 1936). In the Southwest United States cycloths are mixed carbonate siliciclastic packages (Wifeson, 1967). During sea level highstands, the basin was starved, carbonates formed in the shelf area, and siliciclastics were deposited in near shore to terrestrial environments (Wifeson, 1967). During sea level flowstands, the marine carbonates were exposed to meteoric diagenesis and siliciclastics were transported across the exposed shelf into the basin (Wifeson, 1967). Wifeson (1967) termed this cyclical-reciprocal sedimentation. Paleosols formed atop marine carbonates after high-amplitude sea level drops (Gofdstein, 1988; Safler et al., 1994). Gofdstein (1991) used cement stratigraphy and stable isotopes to demonstrate that meteoric diagenesis was confined to the exposed cycle in the Sacramento Mountains of New Mexico. He reasoned that this resulted from the permeability barrier at the base of the cycle, perhaps from the preceding subaerial exposure event. Safler et al. (1994) showed that porosity development in cyclothemic strata was controlled by the duration of exposure. With long-term sea level rise, cycles experienced shorter durations of exposure and enhanced porosity, while with long term sea level drop, exposure was intensified, destroying porosity, cycles are shorter, and there are missed cycles (Safler et al., 1994, 1999).

Building on this foundation, Rasbury et al. (1998, 2000, 1997) tested the potential for U-Pb dating of calcrites produced during subaerial exposure (paleosols). Using the paleosol U-Pb ages in the context of biostratigraphy and cycle stratigraphy, Rasbury et al. (1998) estimated the age of the Carboniferous-Permian boundary to be 301 ± 2 Ma (2 σ). At the time of that publication, the Harland et al. (1990) geological timescale had this boundary at 290 ± 20 Ma (2 σ). Subsequently, Ramezanian et al. (2007) presented high precision zircon ages from the type section in the Ural Mountains and estimated that boundary to be $298.90 \pm 0.31/0.15$ Ma (2 σ), impressively precise and entirely consistent with the U-Pb carbonate age estimate of that boundary. In addition to the paleosol ages, Rasbury et al. (2004) dated neomorphosed aragonite marine cements from the Laborcita Formation in the Sacramento Mountains of New Mexico and obtained an age of 300 ± 3.8 Ma (2 σ). The argument mounds that these marine cements derived from, is approximately two high-frequency cycles before the Carboniferous-Permian boundary (Rasbury et al., 2004), and is thus entirely consistent with the Ramezanian et al. (2007) age estimates for this biostratigraphic interval. Combined, these ages offer an opportunity to consider cycle durations and compare with high-precision dated records in the Donets Basin (Davydov et al., 2010). Davydov et al. (2010) dated 12 ashes and tonstiens in the Donets Basin. Based on these ages, they estimate the duration of cycloths to have been 83 ± 24 ky (Davydov et al., 2010), consistent with the estimate from the southwest United States of 143 ± 64 ky (Rasbury et al., 1998). With the longer term record, Davydov et al. (2010) were also able to consider how these shorter, ~100 ky cycles are packed into ~400 ky cycles. This packing is consistent with the interpretation of Raymond C. Moore, cited in (Wanless and Shepard, 1936). We recalculated boundary ages for both the SW US and the Donets Basin using a Bayesian model (Kefler, 2018) (Fig. 2; Fig. 3). This model produces an age-depth estimate by considering uncertainties on dates and stratigraphic position of dated layers and refines these uncertainties by assuming that dates cannot violate the principles of stratigraphic superposition. Model outputs and uncertainties of undated horizons provide an error envelope that can be used to estimate cycle duration and the ages of biostratigraphic boundaries. The results are similar to those presented in the original studies (Davydov et al., 2010; Rasbury et al., 1998). Rather than a linear model this tests the assumption of equal duration cycles, which would require the slope of each segment is the same within uncertainty. For the case of U-Pb dating of zircons, the errors are small and with the numerous cycles and ages there is little doubt that the cycles represent

Period	Cycles	U-Pb Ages
Pennsylvanian	33	307.26±0.11 Ma
	40	310.55±0.1 Ma
	137	312.01±0.08 Ma
	138	312.23±0.09 Ma
Mississippian	30	313.16±0.06 Ma
	120	314.4±0.06 Ma
	30	328.14±0.1 Ma
	120	342.01±0.1 Ma
	30	345.0±0.08 Ma
	120	345.17±0.07 Ma
		357.26±0.08 Ma

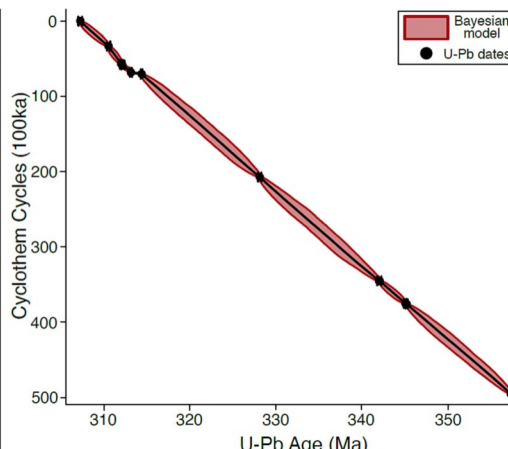


Fig. 2. Simplified stratigraphic column from a cyclothem record in the Donets Basin, Ukraine using cycles as a counting metric, rather than thickness. U-Pb ages measured in zircons from interstratified tuffs; errors reported in 2σ (Davydov et al., 2010). Graph (right) shows U-Pb zircon derived stratigraphic Bayesian age-cycle model for the Donets Basin. Model uses stratigraphic position as a prior to refine uncertainties in dates (Kefler, 2018). Uncertainty envelope represents 95% confidence interval of the age model. (For interpretation of the references to colour in this figure legend, the reader is referred to the web version of this article.)

Period	Cycles	U-Pb Ages
Permian	16	298±1.4 Ma
	16	300±3.8 Ma
Carboniferous	2	298±18 Ma
	13	291±15 Ma
	13	286±14 Ma
	4	303±10 Ma
		306±3 Ma

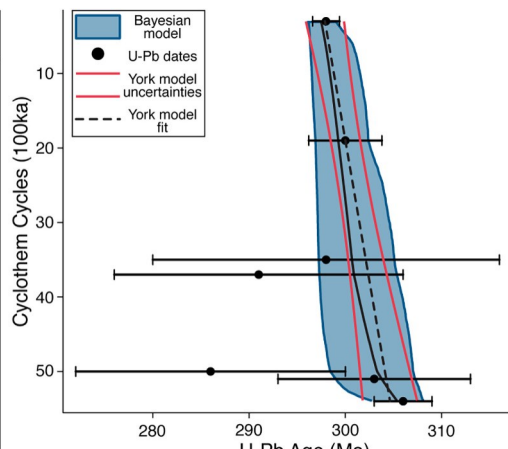


Fig. 3. Simplified stratigraphic column from cyclothem record in the Sacramento Mountains, NM with ages from the Central Basin Platform of the Permian Basin, Texas. U-Pb ages measured in paleosol calcite (Rasbury et al., 1998) and marine cement (Rasbury et al., 2004); errors reported are 2σ . The stratigraphic Bayesian age-depth model uses stratigraphic position as a prior to refine uncertainties in U-Pb paleosol dates (Kefler, 2018). Uncertainty envelope represents 95% confidence interval of age model. The dashed line and bracketing red lines are an age-cycle model derived from linear regression (York and Evensen, 2004) (referred to as York fit) through the U-Pb paleosol data, similar to what Rasbury et al. (1998) used to estimate cycle durations and boundaries. The York fit assumes equal cycle durations. Cycle durations and ages are similar between the models. Errors for the Bayesian model are larger because fit does not assume a linear fit or equal cycle duration. (For interpretation of the references to colour in this figure legend, the reader is referred to the web version of this article.)

equally fine (Fig. 2). In the case of the U-Pb dating of carbonates, the errors are mixed, with some better than 1% errors and others approaching 10% errors. In this case the Bayesian model has inflated errors over a linear fit (York and Evensen, 2004), and may better reflect the real uncertainties since there is no underlying assumption of equal cycle durations. The linear model used by Rasbury et al. (1998) yielded a more precise age for the Carboniferous-Permian boundary (301 ± 2 (2σ)) than the Bayesian model does (300.7 ± 3.95 (2σ)), but the boundary ages are the same within uncertainties (Fig. 3).

3.3. Comparison between isotope dilution and LA U-Pb ages of calcrites

Laser ablation mapping of sample X-1-1 from a core from the Central Basin Platform of the Permian Basin studied by Rasbury et al. (1997) confirms the clear relationship of U with dark brown, organic-rich (smells like crude oil when broken) rhizoflute calcite (Fig. 4). The host rock is lighter brown dolomite, which is easily seen in the Mg map. Si, Sr and Th all have higher concentrations in the dolomite than the calcite (Fig. 4). The $^{238}\text{U}/^{206}\text{Pb}$ is higher in the calcite and the $^{207}\text{Pb}/^{206}\text{Pb}$ is lower in the calcite, consistent with elevated U and ingrowth of ^{206}Pb (Fig. 4).

Laser ablation maps using the Drost approach in Isofite4 (Paton et al., 2011) for extracting and pooling pixels provides a framework for interpreting LA-Ca ages. The pixels correspond to duty cycles. The rate that the sample is moving under the laser is $20 \mu\text{m/s}$ and with the

counting time fit represents close to a second. The spot size is $80 \mu\text{m}$ so the pixels are about 20×80 microns in plan view and nearly $10 \mu\text{m}$ deep. To select for calcite, we chose a criterion of elevated counts of Ca and low counts for Si. This produced 2122 pixels. The pixels were subdivided into 50 pools based on probability on $^{238}\text{U}/^{206}\text{Pb}$. We chose this ratio for pooling because it allows us to achieve the greatest spread in U/Pb without the bias that might be introduced by using the $^{238}\text{U}/^{206}\text{Pb}$. We left out 10% from the lowest and highest ends (as recommended by Drost et al., 2018) and plotted the remaining 40 data points on a Tera-Wasserburg plot using IsoplotR model 3 (Vermeesch, 2018) (Fig. 5). This yields an age of 295 ± 9 Ma (2σ), which is entirely consistent with the published ID-TIMS age of 298.4 ± 1.4 Ma (2σ) (Rasbury et al., 1998), albeit the uncertainty is 10 times higher. To be sure, instruments with higher sensitivity could easily halve the uncertainty we obtained by LA-ICPMS, and it is encouraging that the result is accurate. It is worth discussing how we reduced this data since there are many different approaches that are being taken. In fact, our approach is evolving as we try new things. We used the NIST612 glass as the primary standard. We tuned with NIST612 to maximize signal and minimize oxides and doubly charged ions. We did a final tune with WC-1 using the gas flow and torch position to tune for the $^{238}\text{U}/^{206}\text{Pb}$ ratio, which should be about 23 based on isotope dilution (unpublished and Roberts et al., 2017). For each session, we run WC-1 (Roberts et al., 2017) and Barstow (Rasbury et al., 2021) as secondary standards and we look at the results in Isofite4 to make sure that the ratios on WC-1 are reasonable and that the spread

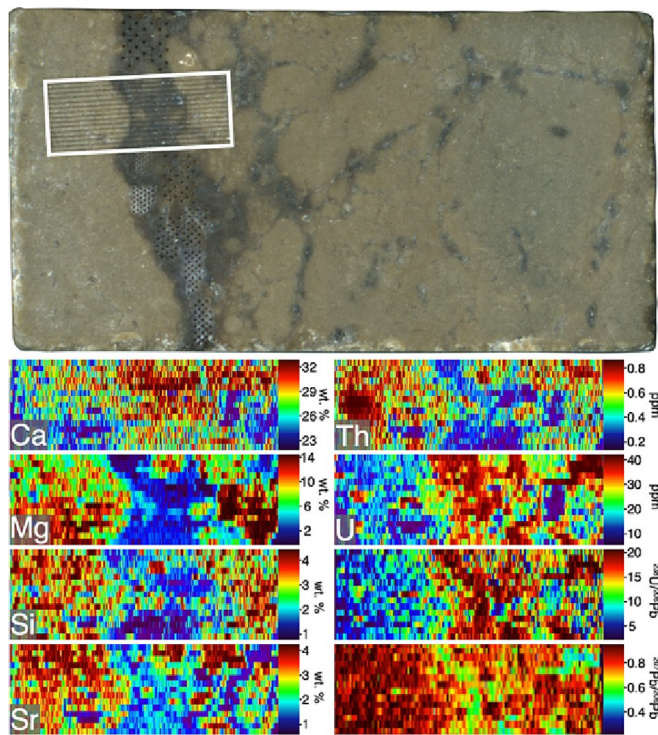


Fig. 4. Slab of sample X-1-1 with a white box showing the LA mapped area. The image is ~ 1 cm across. Element maps below are output from Iolite4 and were used to select pixels for isochron plots. (For interpretation of the references to colour in this figure legend, the reader is referred to the web version of this article.)

in Barstow gives the correct age within uncertainty. For the data presented here, we did not need to make a correction for these secondary standards. That is, the ratios used are the ratios produced using NIST612 as the primary standard and putting the data through the U-Pb Geochronology DRS in Iolite4. This subtracts the baseline, corrects for downhole fractionation (which is negligible with fine scans) and then makes a final correction for fractionation and drift in the signal.

In addition to the calcite, we extracted pixels from the host dolomite. Based on petrography, the dolomite is older than the calcite, which crosscuts the dolomite (Rasbury et al., 1997). Pixels were selected using elevated Mg concentrations. This produced 3900 pixels that were subdivided into 99 bins (the maximum allowed in Iolite4) based on probability on $^{238}\text{U}/^{208}\text{Pb}$. Trimming the low and high 10%, we are left with 78 (throwing out one additional spot with an anomalous U/Pb error) that give an age of 351 ± 13 Ma (2σ) on a Tera-Wasserburg plot (Fig. 5). The sample is from the lower Permian and cannot be older than 300 Ma, and thus this age is far too old even outside the uncertainty. The $^{238}\text{U}/^{208}\text{Pb}$ versus U concentration shows that there are two populations of dolomite. The segment with the lowest U concentrations shows a spread in the $^{238}\text{U}/^{208}\text{Pb}$ without change in the U. This demonstrates that common Pb is more important in this segment than in the other segment, which shows a strong positive correlation between the $^{238}\text{U}/^{208}\text{Pb}$ and U concentration (Fig. 5A). The boundary between these two populations is at a $^{238}\text{U}/^{208}\text{Pb}$ of about 3 (Fig. 5A). Taking only the data points above $^{238}\text{U}/^{208}\text{Pb}$ of 3 ($n = 42$), the age on the Tera-Wasserburg plot is 318 ± 23 Ma. While the nominal age is still slightly old, it is accurate within uncertainty. Without the temporal constraints provided by biostratigraphy and calcite dates, which place the maximum age of this sample at 300 Ma, it would be impossible to interpret the date calculated using all the data as the true sample age. Alternatively, given the prior knowledge of the maximum sample age we could anchor these data to produce an age of 300 Ma. However, this technique prevents the dolomite date from providing a truly

independent age constraint, highlighting the importance of being forthcoming when using anchors and providing context for why the anchor was chosen. In many scenarios, filtering data by other isotopic or elemental ratios could reveal distinct populations that would allow geologists to better assess reasons for inconsistent ages or scatter in data.

3.4. Assessing the potential for U-Pb carbonate ages to predict cyclothem duration

Even the highest age precision will not be able to date all scales of cyclicity, so techniques to extrapolate ages and estimate duration of cycles are needed. Currently, lower calculated uncertainties (precision) suggest a more reliable (accurate) estimation of the real age of a deposit. However, reconstructing the timing of deposition within a stratigraphic sequence is also complicated by the uncertainty imparted by interpolation between age tie-points. Therefore, the precision of deposition age estimates is dependent not only on the precision of individual dates, but also on the number and distribution of ages within the stratigraphic sequence. Age-depth models derived from traditional dating techniques (i.e. zircon U-Pb and sanidine Ar-Ar) benefit from high-precision on individual dates, but are often dependent on the distribution of tephra within the sedimentary sequence, and can suffer from poor stratigraphic coverage. Conversely, dates of carbonate horizons are generally far less precise than zircon or sanidine dates, but carbonates are ubiquitous in the sedimentary record, and, therefore, may offer the opportunity to fill in gaps in chronology, especially as techniques in LACarb evolve towards higher precision and throughput.

To explore how LACarb ages can benefit temporal characterization of cycloths, we simulate the precision and accuracy of deposition age estimates given variable numbers of LACarb dates. This model simulates randomly selecting the stratigraphic positions of N samples within a stratigraphic section containing 200 cycloths of assumed equal duration. In this particular simulation we input cycloths of 100 kyr duration. Uncertainties in the stratigraphic position of the carbonates are set within a range of ± 10 cycles (2σ): a number based on the estimated ability for geologists to place a sample in vertical space within a section with 95% confidence. Uncertainties in carbonate ages are set to a range of ± 9 Myr (2σ), equivalent to 3% standard error for 300 Ma for LACarb analyses. The simulation assumes a normal distribution for the cycle positions and the respective carbonate ages. We then use a linear regression (York fit) that accounts for errors in both x and y variables (York and Evensen, 2004) to simulate our ability to recover the true cycle duration (the slope of the best-fit line) and age distribution along the line. A Monte Carlo simulation repeats this experiment of N LACarb ages, randomly placed within this section, 5000 times. This allows us to calculate (1) the expected standard error for the age of a horizon within the section and (2) the expected standard error for the cycle duration, given N LACarb ages randomly placed within the section. The precision of both cycle duration and horizon age estimate increases with increasing number of U-Pb age tie-points within a sequence (Fig. 6). As the number of LACarb ages increases to above 10 samples, the precision of deposition age estimates for individual stratigraphic horizons approaches 1% (2σ) error (Fig. 6A). Similarly, ~10 LACarb ages allows for estimates of cycle duration of ± 30 kyr (2σ uncertainty), which is better than half a cycle for the 100 kyr cycloths (Fig. 6B).

As LACarb methods and standards continue to improve, greater levels of precision may be possible in the future. To illustrate this scenario, we repeated the simulations by assuming that LACarb analyses could reach 1% 2σ error (dashed curves in Fig. 6a,b). In this case, 15 LACarb ages in a stratigraphic section containing 200 cycloths would allow for cycle duration estimates to ± 9 kyr (2σ).

Using the same approach, but with uncertainties of 0.1 Ma (2σ) for U-Pb zircons, it takes far fewer ages to achieve much better precision for cycle durations (Fig. 6C; D). This experiment provides an example for a single stratigraphic section with the underlying assumption of equal cycle durations. In typical stratigraphic sequences, stratigraphic

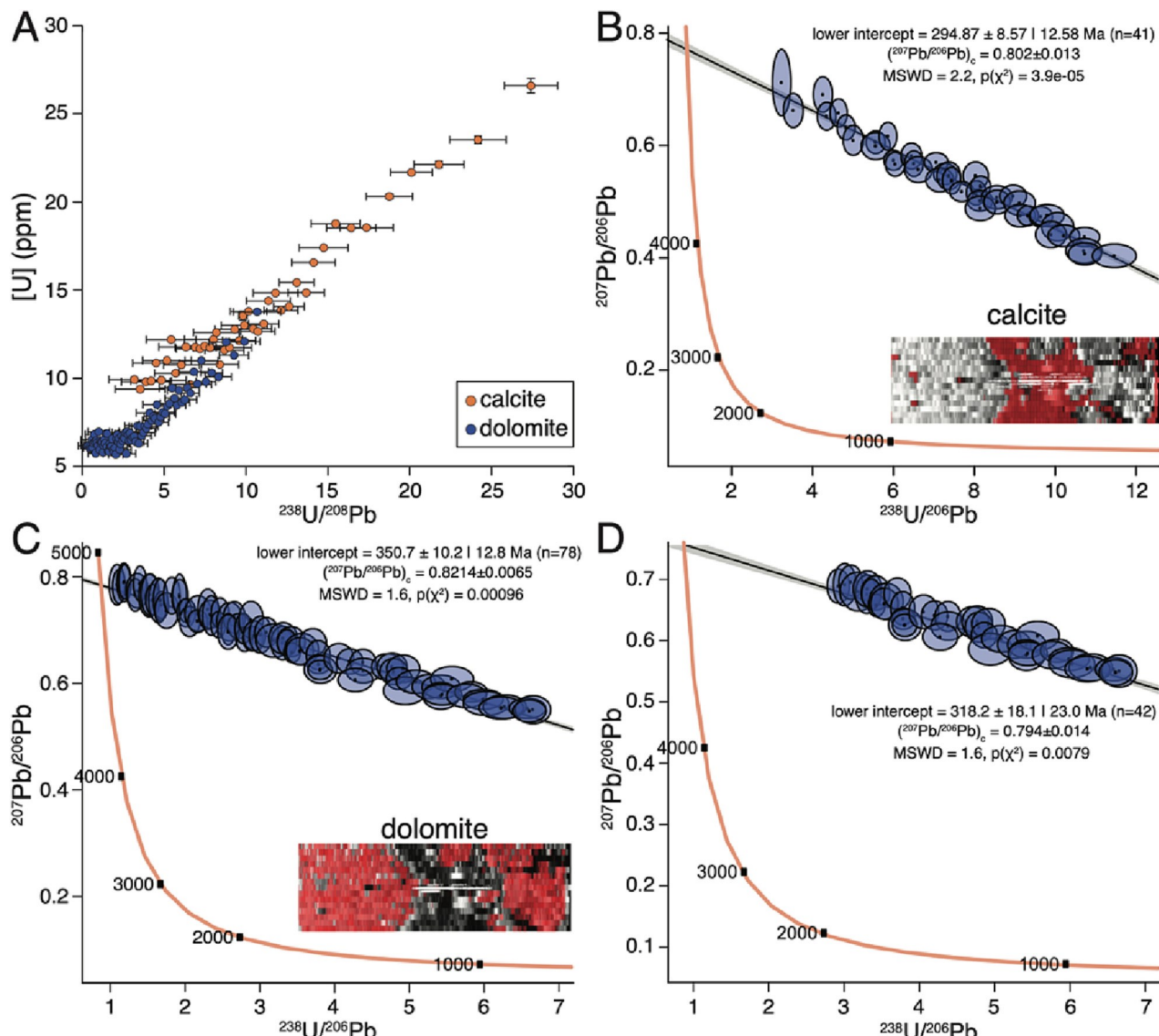


Fig. 5. U-Pb Analyses of calcite and dolomite in sample X-1-1. A. $^{238}\text{U}/^{208}\text{Pb}$ versus U concentration shows a clear difference between calcite, which was selected based on high Ca and low Si, and dolomite, which was selected based on high Mg concentrations. The dolomite shows two domains: the flow end and a near horizontal line showing that the range $^{238}\text{U}/^{208}\text{Pb}$ results from a range of Pb concentrations, while the domain that has higher $^{238}\text{U}/^{208}\text{Pb}$ shows a strong positive relationship between $^{238}\text{U}/^{208}\text{Pb}$ and U concentrations showing that, for this domain, the range is due to the range in U concentrations. B. The inset is a map of the sample with calcite shown by red pixels. The Tera-Wasserburg plot was output from IsoplotR using model 3, and shows data subdivided from the red calcite pixels and pooled based on the $^{238}\text{U}/^{208}\text{Pb}$. C. The inset is a map of the sample with dolomite shown by red pixels. The Tera-Wasserburg plot (as above) shows all the data from the subdivided dolomite pixels. The age derived from these data of 350.7 ± 10.2 is too old. D. Tera-Wasserburg plot derived using only the data above $^{238}\text{U}/^{208}\text{Pb}$ of 3 based on the change of slope in (A). These data give the correct age with uncertainty. (For interpretation of the references to colour in this figure legend, the reader is referred to the web version of this article.)

position is defined by depth of dated layers above the surface, and uncertainty is based on layer thickness estimates. However, when constructing models describing cyclothem ages, we recommend instead to describe the stratigraphic position of dated layers by their cycle position in the section. That is, set the base of the stratigraphic column as cycle 0 and assign a cycle number to each cycle top. Cycle counts are based on careful analysis involving the recognition of cyclothem patterns. We demonstrate this approach both in our reanalysis of cycloths in the Urals and Sacramento Mountains (Fig. 2; Fig. 3), as well as in our idealized cyclothem simulations (Fig. 6). Defining stratigraphic position based on cycles rather than thickness is a reasonable approach because while the packages can have vastly different thicknesses, the cycles are easy to identify, and it is reasonable to assume they are paced by some periodic function such as Milankovitch cycles. However, this approach assumes the number of cycles is known. Boundaries not identified can

mean there are amalgamated cycles. Additionally, cycles with different durations can present similar facies patterns such that extra cycles may be identified. The better constrained the 3-dimensional depositional stratigraphy is known the greater the confidence in cycle counting. Using cycle number (cycle superposition) frees one from applying this to a single section or keeping the measurements to the same depositional position and facies.

The synthetic experiment in Fig. 6 provides the expected precision of recovering 100 kyr cycles in a 200-cycle section. But what if the section contains 200 cycles that involve other Milankovitch cycle durations, such as 18 kyr, 41 kyr, or 400 kyr? Would it be possible to still resolve these cycle durations? To test this, we performed a set of simulations using 200 cycles of constant duration of 18 kyr, 41 kyr, 100 kyr, and 400 kyr, respectively (Table 2). For these simulations we tested just 10 LACarb ages with $3\% 2\sigma$ standard error. We also tested 10 LACarb ages

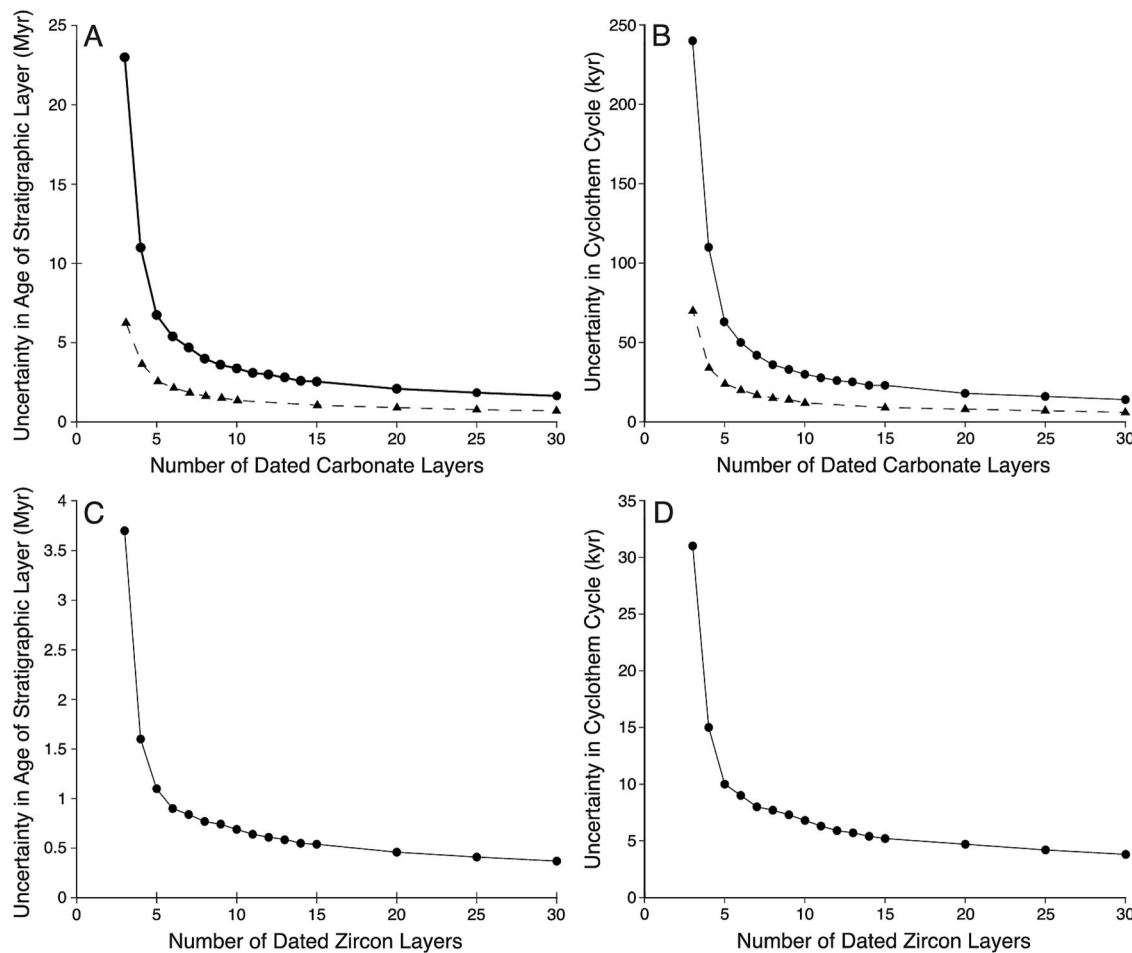


Fig. 6. Simulation of precision of LACarb and tephra derived cyclothem age estimates. A. Monte Carlo simulation of uncertainty in age estimates reported as 2σ absolute standard error on a 310 Myr stratigraphic horizon based on an increasing number of dated carbonate layers in a idealized section containing 200 cycles of 100 kyr duration. Solid line with circular markers shows stratigraphic layer uncertainties derived from LACarb ages with 2σ standard error values of 9 Ma; dashed line with triangle markers shows stratigraphic layer uncertainties derived from LACarb ages with 2σ standard error values of 3 Ma. B. Monte Carlo simulation of uncertainty in cycle duration reported as 2σ absolute standard error on a 100 kyr cyclothem cycle duration based on a variable number of dated carbonate layers in a idealized section. Solid line with circular markers shows cycle duration uncertainties derived from LACarb ages with 2σ standard error values of 9 Ma; dashed line with triangle markers shows cycle duration uncertainties derived from LACarb ages with 2σ standard error values of 3 Ma. C. Monte Carlo simulation of uncertainty in age estimates reported as 2σ absolute standard error on a 310 Myr stratigraphic horizon based on an increasing number of dated tephra deposits with high-precision zircon ages in the same idealized section as for carbonates. D. Monte Carlo simulation of uncertainty in cycle duration reported as 2σ absolute standard error on a 100 kyr cyclothem cycle duration based on a variable number of dated tephra layers in an idealized section. (For interpretation of the references to colour in this figure legend, the reader is referred to the web version of this article.)

Table 2

Simulated achievable age precision of cyclothem cycles paced by different Milankovitch cycles using LACarb. Values assume 10 LACarb ages in a cyclothem made up of 200 cycles.

Cycle Duration (kyr)	2σ Individual Layer Uncertainty (myr)	2σ Cycle Uncertainty (kyr)
10 LACarb ages with ± 9 Ma (2σ) uncertainties in a 200-cycle sequence		
18 kyr	3.34	30
41 kyr	3.3	30
100 kyr	3.4	30
400 kyr	4.7	42
10 LACarb ages with ± 3 Ma (2σ) uncertainties in a 200-cycle sequence		
18 kyr	1.1	10
41 kyr	1.16	10
100 kyr	1.38	12
400 kyr	3.38	29

with the higher precision of 1% 2σ standard error. We find that the standard deviation in cycle duration is essentially the same for all cases, with the 400 kyr cycles yielding slightly larger absolute uncertainties

(Table 2). This near invariance of uncertainties in cycle duration is also the case for the uncertainty in horizon ages. The implication from these findings is that 400 kyr and 100 kyr cycles can be distinguished. However, 18 kyr and 41 kyr cycles cannot be discriminated from one another. On the other hand, higher precision LACarb ages with 1% 2σ standard error yield cycle duration uncertainties of ± 10 kyr (2σ standard error) for the 18 kyr and 41 kyr cycles. Thus, such higher precision LACarb ages will make it possible to resolve the difference between 18 kyr and 41 kyr (Table 2) and allow for the identification of higher frequency cyclothems.

Application of a linear regression and use of cycle number assumes that the cycle duration is the same, on average, throughout the section. This assumption works for making the point in Fig. 6, but we recommend using a Bayesian model on real data. The Bayesian model eliminates the need to assume the cycles are of equal duration and actually tests that assumption. However, the linear modeling provides a powerful predictive tool in planning one's approach to field sampling, and for understanding the limitations of data sets of a certain size. Will five more samples make a large difference in uncertainties or a negligible change?

This approach takes advantage of what we do know about stratigraphic sequences and can be used as a predictive tool to determine the minimum number of cycle age dates needed for lowest age uncertainties. The solution depends on the number of cycles within the given duration of section of interest.

3.5. Using stratigraphic constraints to refine depositional age models

Layering and cycles in carbonates range from years to millions of years. There will always be a limit on what cycle durations can be directly constrained. For using LACarb to date 100ky cycles, which may have attributed to the cycloths, age modeling is required for determining average duration of cycles over a long interval, with age-depth models or age-cycle models. Age-depth models are fraught with uncertainties due to varying layer thicknesses. The thickness of a depositional cycle of any scale will vary greatly through the 3-dimensionalities of a cyclic package. Maintaining the same depositional and facies position from cycle to cycle commonly cannot be done in a single vertical section and requires a well constrained 3-D cycle stratigraphy. To avoid the issue due to depth/thickness variations we recommend applying cycle-age models instead of or in addition to age-depth models. The predictive model in Fig. 6 required the assumption that all cycles are the same duration (whatever that is), and that all the cycles are included. The linear regression method that we use (York and Evensen, 2004) does account, however, for uncertainties in cycle position (2σ standard error of ±10 cycles). Nevertheless, techniques that do not require such assumptions of constant cycle duration, like the Bayesian model of Kefler (2018), are needed.

Refining the uncertainties of stratigraphic age models using the principle of superposition can increase the level of precision on carbonate generated age-stratigraphic models because it utilizes the greater stratigraphic coverage achievable through LACarb to decrease the uncertainty on individual age points (Montano et al., 2022). The idea behind using the constraint of superposition to refine stratigraphic models is that individual dated layers or cycles cannot be older than layers or cycles below them, nor younger than layers above them. Therefore, models can be refined to reject ages that violate the superposition constraint, based on the dates of layers above and below them. Examples of other studies that have utilized this approach for stratigraphic age models include Guex et al. (2012), Haslett and Parnell (2008), and Meyers et al. (2012). The Chron.jfl software uses Bayesian Markov chain Monte Carlo model to refine age-depth estimates with the superposition constraint (Kefler, 2018). The main input parameters for Chron.jfl are stratigraphic age-type points, stratigraphic height, and the respective uncertainties. An example of the use of this model, with a detailed description of the approach can be found in the supplement of (Schoene et al., 2019). Further, while not explored in this review, Chron.jfl can also incorporate estimates for hiatuses in deposition (as detailed in Defino et al. (2019)), which can be useful for defining stratigraphic age models where unconformities are identified by field relationships.

We used Chron.jfl to generate cycle-age models by describing stratigraphic position in terms of cycle numbers. The Chron.jfl model does not assume a constant deposition (or cycle period) rate, but instead allows one to consider details of cycle stacking. That is, changes in slope when this model is used with cycles instead of stratigraphic thickness shows either missing cycles, or perhaps that cycles do not represent the same duration. If one had continuous data, a missing cycle would show up as an offset of the line. With fewer data points, this would show up as a change in slope. For example, in Fig. 2B there is an offset in the curve that occurs where Davydov et al. (2010) recognized missing section in the Donets Basin relative to the Urali based on biostratigraphy.

To further explore the application of statistical fits to age-cycle models of cycloths, we apply Chron.jfl to two modeled stratigraphic columns. One section has 5 randomly generated age type-points and the other has these same 5 points plus an additional 5; age uncertainties are within the range currently expected with LACarb (we anticipate these

uncertainties within 10%) for both sections (Fig. 7). We also apply the linear regression (York and Evensen, 2004) to both sets of data. This experiment is meant to simulate a reasonable estimate of the precision and accuracy of cyclothem age-depth modeling generated by LACarb dated stratigraphic layers and to show the model improvement that comes with a greater number of LACarb dated horizons that are randomly located within the section. With only 5 samples, the application of Chron.jfl provides a higher confidence in model ages than the linear regression (Fig. 7A). However, with 10 LACarb ages, the linear regression predicts a higher confidence level (Fig. 7B). This higher confidence level is likely an artifact of the embedded assumption of constant cycle duration (constant slope) for the linear regression method.

The ability to place a local, 2-dimensional stratigraphic column in a 3-dimensional context, provides a higher confidence level in cycle packaging, including where cycles are amalgamated or eroded. The 3-dimensional framework also offers a natural test of dating the same cycles in different locations. Sequence stratigraphic packages come in many sizes. Most of the underlying processes that could drive these scales of cycles are dependent on the duration of the cycles. Therefore improved age constraints of cycles will advance testing of driving forces. While 3–5% uncertainties on a given boundary provide only a coarse constraint, multiple ages within a section can test the average duration of packages (cycles) and refine our understanding of processes that built them. It is notable that dated records of cycloths appear to point to an approximately 100ky cycle, similar to what is seen in the Paleocene. Prior to age dating a consensus was growing that cycloths were 400ky cycles (Heckel, 2008). While the uncertainty on the average estimates based on carbonates are large, they clearly distinguish cycloths from 400ky cycles. It is clear that LACarb has great potential for refinement of strata ages and for testing the orders of packages within those strata.

4. Suggested best practices for obtaining LACarb dates of sequence stratigraphic units

The application of LACarb dating to place time constraints on the sedimentary rock record is a burgeoning geochronological technique. While previous review papers have covered LACarb methods (e.g. Roberts et al., 2020), we add here notes and suggested best practices for applying LACarb dating to sequence stratigraphy.

I. Field work and sample collection

- Stratigraphic sequences are 3-dimensional bodies that are often incomplete in individual vertical outcrops. Two-dimensional cross sections (i.e., Eros et al., 2012; Montanez, 2022) are better to capture details. However, the goal standard of sample collection, is to collect multiple samples from a single bed or unit in the 3-dimensions of a stratigraphic sequence.

- To expand on point a: It is important to note that each individual stratigraphic section, on average, will have more gaps in deposition than units (Wilson, 1975).

- Due to the ability to statistically refine age-depth models, it often be more important to measure more samples distributed through the section than having fewer high-resolution dates.

II. For sample characterization prior to measuring U–Pb ages:

- Carbonates can readily be altered after initial deposition. Therefore, carbonate U–Pb dating requires constraints on diagenesis of components being dated, cross-cutting reworking relationships and superposition at all scales (i.e. sequences to diagenetic cements).
- It is not necessary to strictly measure unaltered carbonates. For example, most marine cements in the Phanerozoic require pre-existing cavities, and peloids require that sediments have been exposed through erosion. Rather, carbonate U–Pb

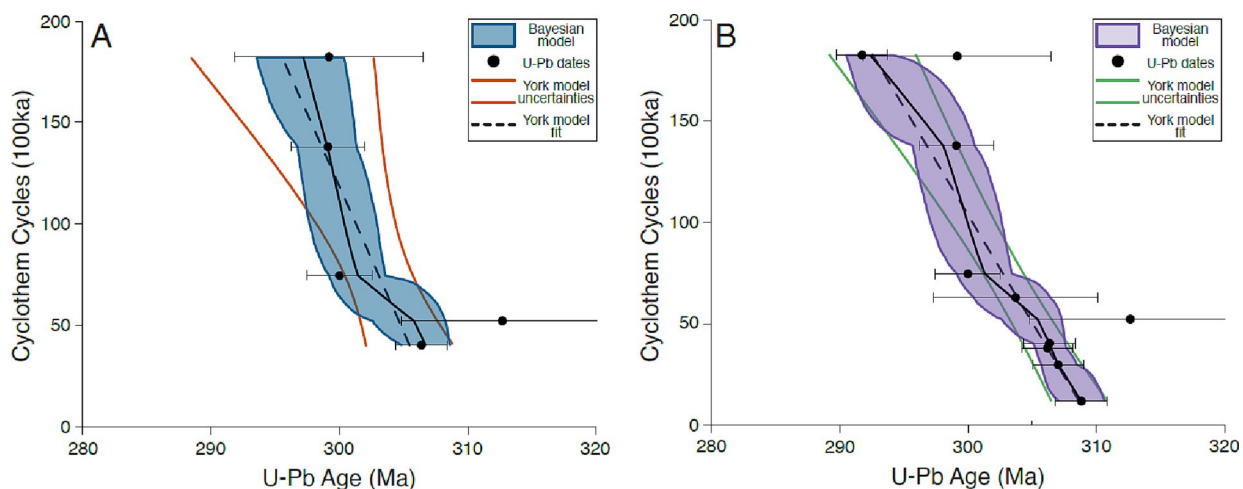


Fig. 7. Idealized LACarb generated age-depth model using Chron.jfl and York fit. A. Five randomly generated LACarb dated stratigraphic horizons. Solid blue line indicates stratigraphic age model generated with Chron.jfl, with 2σ error window indicated by blue envelope. Dashed red line indicates York fit cycle-age model, with 2σ error window shown in red. Age uncertainties reported as 2σ absolute standard error. B. Ten randomly generated LACarb dated stratigraphic horizons. Ages include the 5 dates from A, plus five new dates. Stratigraphic age model derived from Chron.jfl and York fit, as in (A). Uncertainties reported as 2σ absolute standard error. (For interpretation of the references to color in this figure legend, the reader is referred to the web version of this article.)

dating requires careful determination of the individual events recorded in a sample so that age-estimates can be placed in a proper geological context (e.g. Brugaud et al., 2021; Montano et al., 2022).

III. For measuring U-Pb ages and stratigraphic age-depth models:

- It can often save time and resources to determine which, if any, components of a sample have U/Pb ratios suitable for U-Pb dating, prior to making measurements. The easiest method to pre-screen samples is to generate LA maps of high U, low Pb areas.
- Measuring U and Pb from an individual fabric within a sample can be done using a LA map in the Ioffelite4 software, which allows the analyst to select individual pixels within the image based on user-defined criteria (e.g. elemental concentrations, or ratios) (method described in Drost et al., 2018).
- Individual LACarb dates do not need to have the highest possible precision to be useful in defining a stratigraphic age model. The greatest strength offered by carbonate U-Pb dating for adding temporal constraints in sequence stratigraphy is likely to be the ability to generate large numbers of dates for a given section.
- The precision of carbonate derived age-depth models is likely to benefit from the additional constraint of stratigraphic superposition to refine uncertainties on individual dates. Chron.jfl (Kefler, 2018) is a publicly available software that outputs a Bayesian age-depth model incorporating stratigraphic position of dated layers.

5. Conclusions and perspectives

The sedimentary rock record is the primary archive of the evolution of climate and life. The climate record comes from plant and animal fossils and carbon compounds that are preserved in the record that can be used as proxies for environmental conditions. The chemostratigraphic record preserved in marine carbonates not only provides a framework for correlation, but also contains details of the processes and responses to changes. Fossils found within sedimentary sequences are the record of first and last appearances, extinction events, and evolution of animals and plants. These rich archives are deposited in stratigraphic sections, which often do not have recognizable volcanic ash deposits, and can, therefore, be better characterized through the addition of carbonate U-Pb dates.

The stacking pattern of sedimentary strata can also help to unravel details of sea level change and tectonics: processes that respond to and/or drive environmental change. In terrestrial environments changes in flake level or fluvial processes are also tied to climate and tectonics. Testing hypotheses of processes that produce stacking patterns requires age constraints. Correlations between records, particularly marine and terrestrial records is key to understanding these underlying influences. While volcanic ashes are increasingly recognized in the sedimentary record and type sections have increasingly well-defined ages, there remain many uncertainties in correlations which techniques such as U-Pb dating of syn-sedimentary carbonates can help to address.

Declaration of Competing Interest

The authors declare that they have no known competing financial interests or personal relationships that could have appeared to influence the work reported in this paper.

Data availability

Data will be made available on request.

Acknowledgements

This manuscript is dedicated to the late Sam Bowring who initiated Earthtime and was one of the first researchers to test the potential for U-Pb dating of carbonates. Bill Hanson and Bill Meyers' long-term collaboration on isotopes in carbonates launched the U-Pb carbonates work at Stony Brook, and helped set the stage for LACarb. Art Saffer and Bob Goldstein played a central role in establishing the stratigraphic framework for the cycloths and have always been supportive of the U-Pb carbonates work. Randy Parrish is particularly acknowledged for initiating LA ICPMS dating of carbonates. His vision has launched a new era in geochronology. Over the years aspects of this work were funded by NSF, PRF and DOE through various avenues. Katie Wooton, FIRST lab manager is acknowledged for the faster ablation analyses presented here.

Appendix A. Supplementary data

Supplementary data to this article can be found online at <https://doi.org/10.1016/j.earscirev.2023.104495>.

References

Amfliel, A.J., Miffler, D.S., Friedman, G.M., 1973. Incorporation of uranium in modern corals. *Sedimentology* 20, 523–528. <https://doi.org/10.1111/j.1365-3091.1973.tb01629.x>

Antonellifi, M.A., Pester, N.J., Brown, S.T., DePaolo, D.J., 2017. Effect of paleoseawater composition on hydrothermal exchange in midocean ridges. *Proc. Natl. Acad. Sci.* 114, 12413–12418. <https://doi.org/10.1073/pnas.1709145114>.

Bishoff, J.W., Montañez, I.P., Guibranson, E.L., Brenckle, P.L., 2009. The onset of mid-Carboniferous glacio-eustasy: Sedimentological and diagenetic constraints, Arrow Canyon, Nevada. *Palaogeogr. Palaeoecol. Palaeclimatol. Palaecol.* 276, 217–243. <https://doi.org/10.1016/j.palaeo.2009.02.019>.

Bilfinsfuk, P.M., Sharp, W.D., 2003. Rates of late Quaternary normal faulting in Central Tibet from U-series dating of pedogenic carbonate in displaced fluvial gravel deposits. *Earth Planet. Sci. Lett.* 215, 169–186. [https://doi.org/10.1016/S0012-821X\(03\)00374-1](https://doi.org/10.1016/S0012-821X(03)00374-1).

Bilfinsfuk, K., Oskin, M., Fletcher, K., Rockwell, T., Sharp, W., 2012. Assessing the reliability of U-series and 10Be dating techniques on fluvial fans in the Anza Borrego Desert, California. *Quat. Geochronol.* 13, 26–41. <https://doi.org/10.1016/j.quageo.2012.08.004>.

Briigaud, B., Andrieu, S., Blaifte, T., Haufine, F., Barbarand, J., 2021. Calcite-uranium–lead geochronology applied to hardground lithification and sequence boundary dating. *Sedimentology* 68, 168–195. <https://doi.org/10.1111/sed.12795>.

Carroll, A.R., Bohacs, K.M., 1999. Stratigraphic classification of ancient flakes: Balancing tectonic and climatic controls. *Geology* 27, 99. [https://doi.org/10.1130/0091-7613\(1999\)027<99:SCAOLB>2.3.CO;2](https://doi.org/10.1130/0091-7613(1999)027<99:SCAOLB>2.3.CO;2).

Chung, G., Swart, P., 1990. The concentration of uranium in fresh-water vadose and phreatic cements in a Holocene ooid cay: a method of identifying ancient water tables. *J. Sediment. Petrol.* 60, 735–746.

Cofle, J.M., Nienstedt, J., Spataro, G., Rasbury, E.T., Lanzfirotti, A., Cefelstian, A.J., Nifflson, M., Hanson, G.N., 2003. Phosphor imaging as a tool for in situ mapping of ppm levels of uranium and thorium in rocks and minerals. *Chem. Geol.* 193, 127–136. [https://doi.org/10.1016/S0009-2541\(02\)00223-1](https://doi.org/10.1016/S0009-2541(02)00223-1).

Cofle, J.M., Rasbury, E.T., Montañez, I.P., Pedone, V.A., Lanzfirotti, A., Hanson, G.N., 2004. Petrographic and trace element analysis of uranium-rich tufa calcite, mid-Carboniferous Barstow Formation, California, USA: Uranium-rich tufa deposits, California. *Sedimentology* 51, 433–453. <https://doi.org/10.1111/j.1365-3091.2004.00631.x>.

Cofle, J.M., Rasbury, E.T., Hanson, G.N., Montañez, I.P., Pedone, V.A., 2005. Using U-Pb ages of Miocene tufa for correlation in a terrestrial succession, Barstow Formation, California. *Geol. Soc. Am. Bull.* 117, 276. <https://doi.org/10.1130/B25553.1>.

Crowell, J.C., 1978. Gondwanan glaciation, cyclothems, continental positioning, and climate change. *Am. J. Sci.* 278, 1345–1372. <https://doi.org/10.2475/ajs.278.10.1345>.

Davydov, V.I., Crowley, J.L., Schmitz, M.D., Pofleta, V.I., 2010. High-precision U-Pb zircon age calibration of the global Carboniferous time scale and Miflankovitch band cyclicity in the Donets Basin, eastern Ukraine: U-Pb AGE OF THE CARBONIFEROUS AND CYCLICITY. *Geochim. Geophys. Geosyst.* 11. <https://doi.org/10.1029/2009GC002736> n/a-n/a.

Defino, A.L., Dommartin, R., Kefler, C.B., Potts, R., Behrensmeyer, A.K., Beverly, E.J., Kfing, J., Hefif, C.W., Stockecke, M., Brown, E.T., Moerman, J., deMenocal, P., 2019. Chronostratigraphic model of a high-resolution driller core record of the past million years from the Koora Basin, South Kenya Rift: Overcoming the difficulties of variable sedimentation rate and hiatuses. *Quat. Sci. Rev.* 215, 213–231. <https://doi.org/10.1016/j.quascirev.2019.05.009>.

Demicco, R.V., Lowenstein, T.K., Hardife, L.A., Spencer, R.J., 2005. Model of seawater composition for the Phanerozoic. *Geology* 33, 877. <https://doi.org/10.1130/G21945.1>.

Denniston, R.F., Asmerom, Y., Poflyak, V.Y., McNeiffl, D.F., Klaus, J.S., Cofle, P., Budd, A.F., 2008. Caribbean chronostratigraphy refined with U-Pb dating of a Miocene coral. *Geology* 36, 151. <https://doi.org/10.1130/G24280A.1>.

Dickson, J.A.D., 2002. Fossil Echinoderms as Monitor of the Mg/Ca Ratio of Phanerozoic Oceans. *Science* 298, 1222–1224. <https://doi.org/10.1126/science.1075882>.

Dietrich, P., Griffis, N.P., Le Heron, D.P., Montañez, I.P., Kettler, C., Robfin, C., Guifllocheau, F., 2021. Fjord network in Namibia: a snapshot into the dynamics of the late Paleozoic glaciation. *GEOLOGY* 49, 1521–1526. <https://doi.org/10.1130/G49067.1>.

Drost, K., Chew, D., Petrus, J.A., Scholze, F., Woodhead, J.D., Schneidler, J.W., Harper, D.A.T., 2018. An image mapping approach to U-Pb LA-ICP-MS carbonate dating and applications to direct dating of carbonate sedimentation. *Geochim. Geophys. Geosyst.* 19, 4631–4648. <https://doi.org/10.1029/2018GC007850>.

Eiffler, B., Nurfler, P., Kylander-Clerk, A., Wefinberger, R., 2020. Towards in-situ U-Pb dating of dolomites (preprint). SIMS LA-ICP-MS. <https://doi.org/10.5194/ghc-2020-19>.

Eros, J.M., Montañez, I.P., Osfleger, D.A., Davydov, V.I., Nemyrovska, T.I., Pofleta, V.I., Zhyklyay, M.V., 2012. Sequence stratigraphy and onlap history of the Donets Basin, Ukraine: Insights into Carboniferous facies dynamics. *Palaogeogr.* Palaecoflimate. Palaecol. 313–314, 1–25. <https://doi.org/10.1016/j.palaeo.2011.08.019>.

Felding, C.R., 2021. Late Paleozoic cyclothems – a review of their stratigraphy and sedimentology. *Earth-Sci. Rev.* 217, 103612. <https://doi.org/10.1016/j.earscirev.2021.103612>.

Felding, C.R., Frank, T.D., 2015. Onset of the glacio-eustatic signal recording late Paleozoic Gondwanan facies growth: New data from paleotropical East Africa, Scotland. *Palaogeogr. Palaecoflimate. Palaecol.* 426, 121–138. <https://doi.org/10.1016/j.palaeo.2015.03.002>.

Fletcher, K.E.K., Sharp, W.D., Kendriff, K.J., Behr, W.M., Hudnut, K.W., Hanks, T.C., 2010. 230Th/U dating of a late Paleocene fluvial fan along the southern San Andreas fault. *Geol. Soc. Am. Bull.* 122, 1347–1359. <https://doi.org/10.1130/B30018.1>.

Fletcher, K.E.K., Rockwell, T.K., Sharp, W.D., 2011. Late Quaternary slip rate of the southern Elsinore fault, Southern California: Dating offset fluvial fans via $^{230}\text{Th}/\text{U}$ on pedogenic carbonate: ELSINORE FAULT SLIP RATE. *J. Geophys. Res. Earth* 116. <https://doi.org/10.1029/2010JF001701>.

Getty, S.R., Asmerom, Y., Qufin, T.M., Budd, A.F., 2001. Accelerated Paleocene coral extinctions for the Caribbean Basin shown by uranium-lead (U-Pb) dating. *Geology* 29, 639. [https://doi.org/10.1130/0091-7613\(2001\)029<639:APCEIT>2.0.CO;2](https://doi.org/10.1130/0091-7613(2001)029<639:APCEIT>2.0.CO;2).

Gofld, R.D., Cowgill, E., Arrowsmith, J.R., Chen, X., Sharp, W.D., Cooper, K.M., Wang, X.-F., 2011. Faulted terrace risers place new constraints on the late Quaternary slip rate for the central Afly Tagh fault, Northwest Tibet. *Geol. Soc. Am. Bull.* 123, 958–978. <https://doi.org/10.1130/B30207.1>.

Gofld, P.O., Behr, W.M., Rood, D., Sharp, W.D., Rockwell, T.K., Kendriff, K., Saflin, A., 2015. Holocene geologic slip rate for the Banning strand of the southern San Andreas Fault, southern California. *J. Geophys. Res. Solid Earth* 120, 5639–5663. <https://doi.org/10.1002/2015JB012004>.

Gofldstein, R., 1988. Paleosols of Late Pennsylvanian cyclical strata, New Mexico. *Sedimentology*. <https://doi.org/10.1111/j.1365-3091.1988.tb01251.x>.

Gofldstein, R., 1991. Stable isotope signatures associated with paleosols, Pennsylvanian Helder Formation, New Mexico. *Sedimentology* 38, 67–77. <https://doi.org/10.1111/j.1365-3091.1991.tb01855.x>.

Gothmann, A.M., Higgin, J.A., Adkins, J.F., Broecker, W., Farley, K.A., McKeon, R., Stolarski, J., Pflanovsky, N., Wang, X., Bender, M.L., 2019. A Cenozoic record of seawater uranium in fossil corals. *Geochim. Cosmochim. Acta* 250, 173–190. <https://doi.org/10.1016/j.gca.2019.01.039>.

Griffis, N.P., Montañez, I.P., Fedorchuk, N., Isbell, J., Mundifl, R., Vesely, F., Wefinshultz, L., Iannuzzi, R., Guibranson, E., Taboada, A., Pagan, A., Sanbor, M.E., Huyskens, M., Wimpenny, J., Ifinol, B., Yin, Q.-Z., 2019. Isotopes to trace Contrafiting provenance of glacial deposits and ice centers in the west-Central Gondwana. *Palaogeogr. Palaecoflimate. Palaecol.* 531. <https://doi.org/10.1016/j.palaeo.2018.04.020>.

Guex, J., Schoene, B., Bartolfini, A., Spangenberg, J., Schaftegger, U., O'Dogherty, L., Taylor, D., Bucher, H., Atudore, V., 2012. Geochronological constraints on post-extinction recovery of the ammonoids and carbon cycle perturbations during the early Jurassic. *Palaogeogr. Palaecoflimate. Palaecol.* 346–347, 1–11. <https://doi.org/10.1016/j.palaeo.2012.04.030>.

Gulbranson, E.L., Montañez, I.P., Fedorchuk, N., Isbell, J., Mundifl, R., Vesely, F., Wefinshultz, L., Iannuzzi, R., Guibranson, E., Taboada, A., Pagan, A., Sanbor, M.E., Huyskens, M., Wimpenny, J., Ifinol, B., Yin, Q.-Z., 2019. Isotopes to trace Contrafiting provenance of glacial deposits and ice centers in the west-Central Gondwana. *Palaogeogr. Palaecoflimate. Palaecol.* 531. <https://doi.org/10.1016/j.palaeo.2018.04.020>.

Gulbranson, E.L., Montañez, I.P., Schmitz, M.D., Ifimarino, C.O., Isbell, J.L., Marenssi, S.A., Crowley, J.L., 2010. High-precision U-Pb calibration of Carboniferous and clastic history, Pagan Group, NW Argentina. *Geol. Soc. Am. Bull.* 122, 1480–1498. <https://doi.org/10.1130/B30025.1>.

Gvrlitzman, G., Frlfiedman, G., Miffler, D., 1973. Control and distribution of uranium in coral reefs during diagenesis. *J. Sediment. Petrol.* 43, 985–997.

Haglund, D., Frlfiedman, G., Miffler, D., 1969. Effect of fresh water redistribution of uranium in carbonate sediments. *J. Sediment. Petrol.* 39, 1283.

Haff, S.M., Van Gosen, B.S., Paces, J.B., Zieffl, R.A., Breit, G.N., 2019. Calcite-uranium deposits in the Southern High Palains, USA. *Ore Geol. Rev.* 109, 50–78. <https://doi.org/10.1016/j.oregeorev.2019.03.036>.

Haq, B.U., Schutter, S.R., 2008. A Chronology of Paleozoic Sea-Level changes. *Science* 322, 64–68. <https://doi.org/10.1126/science.1116148>.

Hardife, L., 1996. Secular variation in seawater chemistry: an explanation for the coupled secular variation in the mineralogies of marine carbonates and potash evaporites over the past 600 my. *Geology* 24, 279–283. [https://doi.org/10.1130/0091-7613\(1996\)024<279:SVICA>2.3.CO;2](https://doi.org/10.1130/0091-7613(1996)024<279:SVICA>2.3.CO;2).

Harland, W.B., Armstrong, R.L., Cox, A.L., Craig, L.E., Smith, A.G., 1990. *A Geologic Time Scale 1989*. Cambridge University Press, Cambridge.

Haslett, J., Pamefl, A., 2008. A simple monotone process with application to radiocarbon-dated depth chronologies. *J. R. Stat. Soc. Ser. C App. Stat.* 57, 399–418. <https://doi.org/10.1111/j.1467-9876.2008.00623.x>.

Heckel, P.H., 1983. Diagenetic model for carbonate rocks in Midcontinent Pennsylvanian eustatic cyclothems. *J. Sediment. Res.* 53, 733–759. <https://doi.org/10.1130/212F82B0-2B24-11D7-8648000102C1865D>.

Heckel, P.H., 2008. Pennsylvanian cyclothems in Midcontinent North America as far-field effects of waxing and waning of Gondwana ice sheets. In: Special Paper 441: Resolving the Late Paleozoic Ice Age in Time and Space. Geological Society of America, pp. 275–289. [https://doi.org/10.1130/2008.2441\(19\).1](https://doi.org/10.1130/2008.2441(19).1).

Hoareau, G., Claverie, F., Pecheyran, C., Parfissin, C., Grignard, P.-A., Motte, G., Chafifl, O., Giffrid, J.-P., 2021. Direct U-Pb dating of carbonates from micritic-skeletal femtosecond laser ablation inductively coupled plasma mass spectrometry images using robust regression. *Geochronology* 3, 67–87. <https://doi.org/10.5194/ghc-3-67-2021>.

Hoff, J., Jameson, J., Hanson, G., 1995. Application of Pb isotopes to the absolute timing of regional exposure events in carbonate rocks: an example from the Wahoo Formation (Pennsylvanian), Prudhoe Bay, Alaska. *J. Sediment. Res. Sect. C-Sediment. Petrol. Process.* 65, 225–233.

Hoffland, H.D., Horita, J., Seyfried, W.E., 1996. On the secular variations in the composition of Phanerozoic marine potash evaporites. *Geology* 24, 993. [https://doi.org/10.1130/0091-7613\(1996\)024<993:OTS>2.3.CO;2](https://doi.org/10.1130/0091-7613(1996)024<993:OTS>2.3.CO;2).

Hoffita, J., Zimmermann, H., Hoffland, H.D., 2002. Chemical evolution of seawater during the Phanerozoic. *Geochim. Cosmochim. Acta* 66, 3733–3756. [https://doi.org/10.1016/S0016-7037\(01\)00884-5](https://doi.org/10.1016/S0016-7037(01)00884-5).

Horton, D.E., Poulsen, C.J., Montañez, I.P., Difflfichele, W.A., 2012. Eccentricity-paced paleozoic climatic change. *Palaogeogr. Palaecoflimate. Palaecol.* 331–332, 150–161. <https://doi.org/10.1016/j.palaeo.2012.03.014>.

Israelfson, C., Haflifiday, A.N., Buchardt, B., 1996. U-Pb dating of calcite concretions from Cambrian black shales and the Phanerozoic lime scale. *Earth Planet. Sci. Lett.* 141, 153–159. [https://doi.org/10.1016/0016-821X\(96\)00071-4](https://doi.org/10.1016/0016-821X(96)00071-4).

Keffler, C.B., 2018. CHron.jl: a Bayesian framework for integrated eruption age and age-depth modeling.

Kerans, C., Tinker, S.W. (Eds.), 1997. Sequence Stratigraphy and Characterization of Carbonate Reservoirs. SEPM (Society for Sedimentary Geology). <https://doi.org/10.2110/srn.97.40>.

Kurumada, Y., Aoki, S., Aoki, K., Kato, D., Saneyoshi, M., Tsogtbaatar, K., Wifindley, B.F., Ishigaki, S., 2020. Calcite U-Pb age of the Cretaceous vertebrate-bearing Bayn Shire Formation in the Eastern Gobi Desert of Mongolia: Usefulness of calcite for age determination. *Terra Nova* 32, 246–252. <https://doi.org/10.1111/ter.12456>.

Lahoud, J.A., Miffler, D.S., Friedman, G.M., 1966. Relationship between depositional environment and uranium concentration of molluscan shells. *J. Sediment. Res.* 36, 541–547. <https://doi.org/10.1306/74D71505-2B21-11D7-8648000102C1865D>.

Langford, F.F., 1974. A Supergene Origin for Vein-Type Uranium Ores in the Light of the Western Australian Calcite-Carnotite Deposits. *Econ. Geol.* 69, 516–526. <https://doi.org/10.2113/gsgeon.69.4.516>.

Lawson, M., Sfitgreaves, J., Rasbury, T., Wooton, K., Esch, W., Marcon, V., Henares, S., Konstantinou, A., Kneifler, E., Gombosi, D., Torres, V., Sifila, A., Alevato, R., Alevato, M., Becker, S., Eifler, J., 2022. New age and trace element constraints on the Aptian pre-salt carbonates of the central South Atlantic. *GSA Bufl.* <https://doi.org/10.1130/B36378.1>.

Li, Q., Parrish, R.R., Horstwood, M.S.A., McArthur, J.M., 2014. U-Pb dating of cements in Mesozoic ammonites. *Chem. Geol.* 376, 76–83. <https://doi.org/10.1016/j.chemgeo.2014.03.020>.

Lowenstein, T.K., 2001. Oscillations in Phanerozoic Seawater Chemistry: evidence from fluid inclusion. *Science* 294, 1086–1088. <https://doi.org/10.1126/science.1064280>.

Luczaj, J.A., Gofldstefin, R.H., 2000. Diagenesis of the lower Permian Kridian Member, Southwest Kansas, U.S.A.: Fluid-Inclusion, U-Pb, and Fission-Track evidence for Reflux Dismalization during latest Permian Time. *J. Sediment. Res.* 70, 762–773. <https://doi.org/10.1306/2DC04936-0E47-11D7-8643000102C1865D>.

Meyers, S.R., Sfiewert, S.E., Sfigner, B.S., Sageman, B.B., Condon, D.J., Obradovich, J.D., Jicha, B.R., Sawyer, D.A., 2012. Intercomparison of radiotritopic and astrochronological time scales for the Cenomanian-Turonian boundary interval, Western Interior Basin, USA. *Geology* 40, 7–10. <https://doi.org/10.1130/G32261.1>.

Montañez, I.P., 2022. Current synthesis of the penultimate facies and its imprint on the Upper Devonian through Permian stratigraphic record. *Geol. Soc. Lond. Spec. Publ.* 512, 213–245. <https://doi.org/10.1144/SP512-2021-124>.

Montañez, I.P., Tabor, N.J., Niemeyer, D., Difflchele, W.A., Frank, T.D., Pfeiffer, C.R., Isbell, J.L., Bifgenheier, L.P., Rygg, M.C., 2007. CO₂-Forced Climate and Vegetation Instability during late Paleozoic Deglaciation. *Science* 315, 87–91. <https://doi.org/10.1126/science.1134207>.

Montano, D., Gasparrini, M., Gerdes, A., Della Porta, G., Aiflert, R., 2021. In-situ U-Pb dating of Ries Crater calcareous carbonates (Miocene, South-West Germany): implications for continental carbonate chronostratigraphy. *Earth Planet. Sci. Lett.* 568. <https://doi.org/10.1016/j.epsl.2021.117011>.

Montano, D., Gasparrini, M., Rohafis, S., Aiflert, R., Gerdes, A., 2022. Depositional age models in facies systems from zircon and carbonate U-Pb geochronology. *Sedimentology* 69, 2507–2534. <https://doi.org/10.1111/sed.13000>.

Moarath, S., Taylor, P.N., Orpen, J.L., Treloar, P., Wifison, J.F., 1987. First direct radiometric dating of Archaean stromatolitic limestone. *Nature* 326, 865–867. <https://doi.org/10.1038/326865a0>.

Morad, S., Kettler, J.M., 2013. De Ros. In: L.F. (Ed.), Linking Diagenesis to Sequence Stratigraphy: Morad/Linking Diagenesis to Sequence Stratigraphy. John Wiley & Sons, Inc, West Sussex, UK. <https://doi.org/10.1002/9781118485347>.

Paton, C., Heflifrom, J., Paufl, B., Woodhead, J., Herget, J., 2011. Ioffite: Freeware for the visualization and processing of mass spectrometric data. *J. Anal. At. Spectrom.* 26, 2508. <https://doi.org/10.1039/c1ja10172b>.

Picciione, G., Blaflburn, T., Tufcacy, S., Rasbury, E.T., Hafin, M.P., Ibarra, D.E., Methner, K., Blafling, C., Cheney, B., Northrup, P., Lficht, K., 2022. Subglacial precipitation record Antarctic ice sheet response to late Pliocene millennial climate cycles. *Nat. Commun.* 13, 5428. <https://doi.org/10.1038/s41467-022-33009-1>.

Pofonton, M.A., Chew, D.M., Ovtcharova, M., Deflcambe, B., Sevastopulo, G.D., 2021. Uranium-lead dates from lithic (mudflle Vfsean) bentonites of the Namur-Dinant Basin, Belgium. *Newsl. Stratigr.* 54, 317–334. <https://doi.org/10.1127/nos/2021/0622>.

Pomar, L., Hafllock, P., 2008. Carbonate facies: a conundrum in sedimentary geology. *Earth-Sci. Rev.* 87, 134–169. <https://doi.org/10.1016/j.earscirev.2007.12.002>.

Ramezanji, J., Schmitz, M.D., Davydov, V.I., Bowring, S.A., Snyder, W.S., Northrup, C.J., 2007. High-precision U-Pb zircon age constraints on the Carboniferous-Permian boundary in the southern Urals stratotype. *Earth Planet. Sci. Lett.* 256, 244–257. <https://doi.org/10.1016/j.epsl.2007.01.032>.

Rasbury, E.T., Cofle, J.M., 2009. Directly dating geological events: U-Pb dating of carbonates. *Rev. Geophys.* 47, RG3001. <https://doi.org/10.1029/2007RG000246>.

Rasbury, E.T., Hanson, G.N., Meyers, W.J., Siffler, A.H., 1997. Dating of the time of sedimentation using U-Pb ages for paleosol calcite. *Geochim. Cosmochim. Acta* 61, 1525–1529. [https://doi.org/10.1016/S0016-7037\(97\)00043-4](https://doi.org/10.1016/S0016-7037(97)00043-4).

Rasbury, E., Hanson, G., Meyers, W., Hofst, W., Gofldstefin, R., Siffler, A., 1998. U-Pb dates of paleosols: Constraints on late Paleozoic cycle durations and boundary ages. *Geology* 26, 403–406. [https://doi.org/10.1130/0091-7613\(1998\)026<403:UPDOPC>2.3.CO;2](https://doi.org/10.1130/0091-7613(1998)026<403:UPDOPC>2.3.CO;2).

Rasbury, E.T., Meyers, W.J., Hanson, G.N., Gofldstefin, R.H., Siffler, A.H., 2000. Relationship of Uranium to Petrography of Calcite Paleosols with Application to Precisely Dating the Time of Sedimentation. *J. Sediment. Res.* 70, 604–618. <https://doi.org/10.1306/2DC0492B-0E47-11D7-8643000102C1865D>.

Rasbury, E.T., Ward, W.B., Hemming, N.G., Ifi, H., Difflson, J.A.D., Hanson, G.N., Major, R.P., 2004. Concurrent U-Pb age and seawater 87Sr/86Sr value of a marine cement. *Earth Planet. Sci. Lett.* 221, 355–371. [https://doi.org/10.1016/S0016-821X\(04\)000105-0](https://doi.org/10.1016/S0016-821X(04)000105-0).

Rasbury, E.T., Gfierflowski-Kordesch, E.H., Cofle, J.M., Sookdeo, C., Spataro, G., Nienhuis, J., 2006. Calcite cement stratigraphy of a nonpedogenic calcite fin the Triassic New Haven Arkose (Newark Supergroup), fin: Paleoenvironmental Record and Applications of Calcite and Paleoflurine Carbonates. *Geol. Soc. Am. https://doi.org/10.1130/2006.2416(13)*.

Rasbury, E.T., Present, T.M., Northrup, P., Tappero, R.V., Lanzfiotti, A., Cofle, J.M., Wooton, K.M., Hatton, K., 2021. Tools for uranium characterization in carbonate samples: case studies of natural U-Pb geochronology reference materials. *Geochronology* 3. <https://doi.org/10.5194/gchron-3-1-2021>.

Read, J.F., Kerans, C., Weber, L.J., Sarg, J.F., Wifight, F.M. (Eds.), 1995. Miflankovitch Sea-level Changes, Cycles, and Reservoirs on Carbonate Platforms in Greenhouse and Ice-House Worlds. SEPM (Society for Sedimentary Geology). <https://doi.org/10.2110/srn.95.35>.

Reeder, R.J., Nugent, M., Lamble, G.M., Tafit, C.D., Morris, D.E., 2000. Uranium Incorporation into Calcite and Aragonite: XAFS and Luminescence Studies. *Environ. Sci. Technol.* 34, 638–644. <https://doi.org/10.1021/es990981j>.

Roberts, N.M.W., Hoofsworth, R.E., 2022. Timestcales of faulting through calcite geochronology: a review. *J. Struct. Geol.* 158. <https://doi.org/10.1016/j.jsg.2022.104578>.

Roberts, N.M.W., Rasbury, E.T., Parrish, R.R., Smifit, C.J., Horstwood, M.S.A., Condon, D.J., 2017. A calcite reference material for LA-ICP-MS U-Pb geochronology: Calcite RM for LA-ICP-MS U-Pb dating. *Geochim. Geophys. Geosyst.* 18, 2807–2814. <https://doi.org/10.1002/2016GC006784>.

Roberts, N.M.W., Drost, K., Horstwood, M.S.A., Condon, D.J., Chew, D., Drake, H., Miflowski, A.E., McLean, N.M., Smye, A.J., Wifker, R.J., Haslam, R., Hodson, K., Imber, J., Beaufoin, N., Lee, J.K., 2020. Laser ablation inductively coupled plasma mass spectrometry (LA-ICP-MS) U-Pb carbonate geochronology: strategies, progress, and implications. *Geochronology* 2, 33–61. <https://doi.org/10.5194/gchron-2-33-2020>.

Rochin-Bañaga, H., Davis, D.W., Schwennicke, T., 2021. First U-Pb dating of fossilized soft tissue using a new approach to paleontological chronometry. *Geology* 49, 1027–1031. <https://doi.org/10.1130/G48386.1>.

Rockwell, T.K., Masana, E., Sharp, W.D., Štěpánčková, P., Ferrater, M., Mertz-Kraus, R., 2019. Late Quaternary slip rates for the southern Elsinoe fault in the Coyote Mountains, southern California from analysis of alluvial fan landforms and cleft provenance, soft and U-series ages of pedogenic carbonate. *Geomorphology* 326, 68–89. <https://doi.org/10.1016/j.geomorph.2018.02.024>.

Ross, C.A., Ross, J.R.P., 1985. Late Paleozoic depositional sequences are synchronous and worldwide. *Geology* 13, 194. [https://doi.org/10.1130/0091-7613\(1985\)13-194:LPDSAS>2.0.CO;2](https://doi.org/10.1130/0091-7613(1985)13-194:LPDSAS>2.0.CO;2).

Siffler, A., Difflson, J., Boyd, S., 1994. Cycle stratigraphy and porosity in Pennsylvanian and lower Permian shelf limestones, Eastern Central Basin Platform, Texas. *AAPG Bufl.* 78, 1820–1842.

Siffler, A.H., Difflson, J.A.D., Rasbury, E.T., Ebato, T., 1999. Effects of Long-Term Accommodation Change on Short-Term Cycles, Upper Paleozoic Platform Limestones, West Texas, fin: advances in Carbonate Sequence Stratigraphy. *Application to Reservoirs, Outcrops and Models. SEPM Society for Sedimentary Geology.* <https://doi.org/10.2110/pec.99.11.0227>.

Schoene, B., Eddy, M.P., Samperton, K.M., Keffler, C.B., Keffler, G., Adatte, T., Khadri, S.F. R., 2019. U-Pb constraints on pulsed eruption of the Deccan Traps across the end-Cretaceous mass extinction. *Science* 363, 862–866. <https://doi.org/10.1126/science.aau2422>.

Schroeder, J.H., Miffler, D., Friedman, G., 1970. Uranium distribution in recent skeletal carbonates. *J. Sediment. Petrol.* 40, 672–681.

Sharp, W.D., Ludwig, K.R., Chadwick, O.A., Amundson, R., Gfaser, L.L., 2003. Dating fluvial terraces by ²³⁰Th/U on pedogenic carbonate, Wiflow River Basin, Wyoming. *Quat. Res.* 59, 139–150. [https://doi.org/10.1016/S0033-5894\(03\)00003-6](https://doi.org/10.1016/S0033-5894(03)00003-6).

Smifit, L.B., Fred Read, J., 2000. Rapid onset of late Paleozoic glaciation on Gondwana: evidence from Upper Mississippian strata of the Midcontinent, United States. *Geology* 28, 279–282. [https://doi.org/10.1130/0091-7613\(2000\)028<279:ROOLPG>2.3.CO;2](https://doi.org/10.1130/0091-7613(2000)028<279:ROOLPG>2.3.CO;2).

Stanley, S.M., Hardie, L.A., 1998. Secular oscillations in the carbonate mineralogy of reef-builders and sediment-producing organisms driven by tectonically forced shifts in seawater chemistry. *Palaeogeogr. Palaeoclimatol. Palaeoecol.* 144, 3–19. [https://doi.org/10.1016/S0031-0182\(98\)00109-6](https://doi.org/10.1016/S0031-0182(98)00109-6).

Steuber, T., Vefizer, A., 2002. Phanerozoic record of plate tectonic control of seawater chemistry and carbonate sedimentation. *Geology* 30, 1123–1126. [https://doi.org/10.1130/0091-7613\(2002\)030<1123:PROTC>2.0.CO;2](https://doi.org/10.1130/0091-7613(2002)030<1123:PROTC>2.0.CO;2).

Sumner, D.Y., Bowring, S.A., 1996. U-Pb geochronologic constraints on deposition of the Campbell Island Subgroup, Transvaal Supergroup, South Africa. *Precambrian Res.* 79, 25–35. [https://doi.org/10.1016/0301-9268\(95\)00086-0](https://doi.org/10.1016/0301-9268(95)00086-0).

Vafif, P.R., Miflchum, R.M., Thompson, S., 1977. Seismic Stratigraphy and Global Changes of Sea Level, Part 3: Refraction Changes of Sea Level from Coastal Onlap¹. In: Seismic Stratigraphy — Applications to Hydrocarbon Exploration. American Association of Petroleum Geologists. <https://doi.org/10.1306/M26490C5>.

Van Wagoner, J.C., Posamentier, H.W., Miflchum, R.M., Vafif, P.R., Sarg, J.F., Loutit, T.S., Hardenbol, J., 1988. An overview of the fundamentals of sequence stratigraphy and key definitions. In: Wifflus, C.K., Hastings, B.S., Posamentier, H., Wagoner, J.V., Ross, C.A., Kendal, C.G.S.C. (Eds.), *Sea-Level Changes: An Integrated Approach*.

SEPM Society for Sedimentary Geology, p. 0. <https://doi.org/10.2110/pec.88.01.0039>.

Vermeesch, P., 2018. IsoplotR: a free and open toolbox for geochronology. *Geosci. Front.* 9, 1479–1493. <https://doi.org/10.1016/j.gsf.2018.04.001>.

Wang, Z.S., Rasbury, E.T., Hanson, G.N., Meyers, W.J., 1998. Using the U-Pb system of calcrites to date the time of sedimentation of clastic sedimentary rocks. *Geochim. Cosmochim. Acta* 62, 2823–2835. [https://doi.org/10.1016/S0016-7037\(98\)00201-4](https://doi.org/10.1016/S0016-7037(98)00201-4).

Wanless, H.R., Shepard, F.P., 1936. Sea level and climatic changes related to plate tectonics. *Geol. Soc. Am. Bull.* 47, 1177–1206. <https://doi.org/10.1130/GSAB-47-1177>.

Wilson, J.L., 1967. Cyclical and Reciprocal Sedimentation in Virginian Strata of Southern New Mexico. *Geol. Soc. Am. Bull.* 78, 805–818.

Wilson, J.L., 1975. Carbonate Facies in Geologic History. Springer New York, New York, NY. <https://doi.org/10.1007/978-1-4612-6383-8>.

Winter, B.L., Johnson, C.M., 1995. U-Pb dating of a carbonate subaerial exposure event. *Earth Planet. Sci. Lett.* 131, 177–187. [https://doi.org/10.1016/0012-821X\(95\)00026-9](https://doi.org/10.1016/0012-821X(95)00026-9).

Woodhead, J., Pfickerling, R., 2012. Beyond 500 ka: Progress and prospects in the U-Pb chronology of speleothems, and their application to studies in paleoclimate, human evolution, biodiversity and tectonics. *Chem. Geol.* 322–323, 290–299. <https://doi.org/10.1016/j.chemgeo.2012.06.017>.

Woodhead, J., Hefflstrom, J., Maas, R., Drysdale, R., Zanchetta, G., Devine, P., Taylor, E., 2006. U-Pb geochronology of speleothems by MC-ICPMS. *Quat. Geochronol.* 1, 208–221. <https://doi.org/10.1016/j.quageo.2006.08.002>.

Woodhead, J., Hefflstrom, J., Pfickerling, R., Drysdale, R., Paull, B., Bajo, P., 2012. U and Pb variabilities in older speleothems and strategies for their chronology. *Quat. Geochronol.* 14, 105–113. <https://doi.org/10.1016/j.quageo.2012.02.028>.

Wright, V.P., Vanstone, S.D., 2001. Onset of late Paleozoic glacio-eustasy and the evolving climates of low latitude areas: a synthesis of current understanding. *J. Geol. Soc.* 158, 579–582. <https://doi.org/10.1144/jgs.158.4.579>.

York, D., Evensen, N.M., Martinez, M.L., De Basabe Delgado, J., 2004. Unfitted equations for the slope, intercept, and standard errors of the best straight line. *Am. J. Phys.* 72, 367–375. <https://doi.org/10.1119/1.1632486>.